Thermal/Hydraulic Analysis Research Program Quarterly Report January – March 1984 Volume 1 of 4

S. L. Thompson

8408100147 840731
PDR NUREG
CR-3820 R   PDR

Prepared for
U. S. NUCLEAR REGULATORY COMMISSION

SF 2900-Q(6-82)

THERMAL/HYDRAULIC ANALYSIS RESEARCH PROGRAM
QUARTERLY REPORT JANUARY-MARCH 1984
Volume 1 of 4

S. L. Thompson, Person in Charge

Date Published: June 1984

DA Dahlgren
_____
Manager, Reactor Systems Test and Analysis Department

_____
Director, Nuclear Fuel Cycle Programs

Sandia National Laboratories
Albuquerque, NM 87185
Operated by
Sandia Corporation
for the
U. S. Department of Energy

LIST OF CONTRIBUTORS

Lawrence D. Buxton

Rupert K. Byers

Dean Dobranich

Mildred G. Elrick

Lubomyra Nadia Kmetyk

Andrew C. Peterson

TABLE OF CONTENTS

LIST OF FIGURES

LIST OF TABLES

SUMMARY STATUS REPORT

The TRAC-PF1/MOD1 independent assessment program at Sandia National Laboratories (SNLA) is part of a multi-faceted effort sponsored by the Nuclear Regulatory Commission (NRC) to determine the ability of various systems codes to predict the detailed thermal/hydraulic response of LWRs during accident and off-normal conditions. This program is a successor to the RELAP5/MOD1 independent assessment project underway at Sandia for the last two years.

The TRAC-PF1/MOD1 code [1] will be assessed against data from various integral and separate effects experimental test facilities, and the calculated results will also be compared with results from our previous RELAP5/MOD1 independent assessment analyses whenever possible.

The first quarter of FY84 marked the beginning of the TRAC-PF1/MOD1 independent assessment project at SNLA. The code was obtained from Los Alamos National Laboratory (LANL) in October, and brought up on both our Cyber-76 and Cray-1S computers. The assessment matrix was formalized, several TRAC nodalizations for the various facilities required were developed, and limited calculations were begun, all described in the last quarterly. [2] During this quarter, more nodalizations were developed and calculations begun, and the first PF1/MOD1 assessment analysis was completed.

The results for the B&W once-through steam generator tests 28 and 29 [3] indicate that TRAC can accurately calculate the major global parameters measured during the steady state test such as primary side ΔT, secondary side exit temperature, secondary side inventory, and boiler Δp; the dryout elevation, however, was underpredicted. (This was also a problem observed during our the RELAP5 assessment of the same tests.) The LOFW transient response could be accurately calculated by TRAC (or RELAP5) provided the correct steady state conditions were achieved.

Two methods of modelling the pressure losses associated with abrupt area changes in the form of orifices were tested: the automatic form loss option and the use of user-input K factors. Both methods were found to work satisfactorily; however, it was necessary to input a vena contracta area instead of the actual flow area when using the automatic form loss option. A noding study indicated that good agreement with experimental data could be achieved using 51 mesh cells (compared to 85 for the base, or detailed model) but that using 33 mesh cells produced less satisfactory results.

1.0 INTRODUCTION

The TRAC-PF1/MOD1 independent assessment program at Sandia National Laboratories in Albuquerque (SNLA) is part of a multi-faceted effort sponsored by the Nuclear Regulatory Commission (NRC) to determine the ability of various systems codes to pre-dict the detailed thermal/hydraulic response of LWRs during accident and off-normal conditions. This program is a successor to the RELAP5/MOD1 independent assessment project performed at Sandia during FY82 and FY83.

The TRAC-PF1/MOD1 code [1] will be assessed against data from various integral and separate effects experimental test facili-ties. The assessment matrix was formalized during the last quarter, and is shown in Table 1.1. The calculated results will also be compared with results from our previous RELAP5/MOD1 independent assessment analyses whenever possible. A few of the tests in our TRAC-PF1/MOD1 matrix (i.e., the LOFT L2-5 and LOBI A1-04R large break tests, the PKL ID1 natural circulation test series and the B&W OTSG separate effects tests) were also in our RELAP5/MOD1 assessment matrix, and will allow such cross-comparison.

The first quarter of FY84 marked the beginning of the TRAC-PF1/MOD1 independent project at SNLA. The code was obtained from Los Alamos National Laboratory in October 1984, and brought up on both our CDC Cyber-76 and Cray-1S computers; TRAC nodali-zations for the PKL and B&W OTSG facilities were developed and calculations begun, as described in the last quarterly [2]. These tests were chosen as the starting point because we had reasonably complete facility and test documentation from our RELAP5 assess-ment project, and we wanted some PF1/MOD1 experience with rela-tively simpler tests before beginning full integral system analyses such as for LOFT and Semiscale.

During this quarter, a number of code problems were found in the course of the various assessment calculations, summarized in Section 2.1. Of the calculations begun last quarter, the B&W OTSG analyses have been completed and the PKL natural circulation analyses are continuing, as described in Sections 2.2 and 2.3, respectively. Work began on both the new (to code assessment) Bankoff/Northwestern University condensing horizontal stratified flow and the Delft University of Technology NEPTUNUS pressurizer separate effects tests, with results given respectively in Sections 2.4 and 2.5. A nodalization and steady state calculation were completed for LOBI large break test A1-04R, presented in Section 2.6, and a nodalization was developed for Semiscale intermediate break test S-IB-3, as shown in Section 2.7.

Table 1.1   TRAC-PF1/MOD1 FY84 Assessment Matrix

Test	Scenario
LOFT LP-FW-1	Loss-of-Feedwater
LOFT LP-SB-1	Small Break
LOFT L2-5	Large Break
Semiscale S-IB-3	Intermediate Break (21.7%)
Semiscale S-SF-3,5	1 Steam Line, 1 Feed Line Break
Semiscale S-SG-?	2 Steam Generator Tube Ruptures
Semiscale S-PL-3	Loss-of-Power
PKL ID1 Series	Natural Circulation
LOBI A1-04R	Large Break
LOBI B-R1M	Intermediate Break (25%)
Flecht Seaset 31504	Reflood
Flecht Seaset 31701	Reflood
B&W OTSG 28/29	Loss-of-Feedwater
Flecht Seaset 8	Natural Circulation
Neptunus Y05	Pressurizer Behavior
Dartmouth	3-Tube CCFL
Bankoff	Condensation
Bankoff	Multi-Tube CCFL

2.0 TRAC-PF1/MOD1 ASSESSMENT

2.1 Code Status

Three sets of updates to TRAC-PF1/MOD1, containing the coding to allow many additional signal and control block variables, were received from LANL during the quarter. Because these updates were not yet available on LANL's "user liaison" VAX node, they were taken from Bob Steinke's personal file area on LANL's main computer system. (We pursued use of these new, unreleased code updates primarily because of our analyses of the Northwestern University separate effects tests which were initiated this quarter. Interpretation of those particular analyses involved detailed study of a large number of calculated parameters not normally available as TRAC output quantities.)

These signal and control variable updates from LANL, plus a local modification to allow plotting of the new variables with Sandia's plot program, were incorporated into Version 11.1 of TRAC to create a new production version of TRAC at Sandia. Several problems were encountered when first trying to use the new signal variables, but we resolved those problems after several telephone discussions with Steinke which resulted in additional updates.

Other modifications to Sandia's implementation of TRAC-PF1/MOD1, Version 11.1, were also made during the quarter. Some of the updates were those informally obtained from Frank Addesio during the 12/7/83 TRAC workshop; they allow both sides of a heat slab in the steam generator to "talk" to the same hydro-dynamic cell. Other updates developed by Sandia were made: to force a graphics dump at the time of the final restart dump, to write the times of the graphic dumps to TAPE59, and to correct several printout errors present during the initial edit after restarting a calculation.

Additional work was also done this quarter on our version of the TRAC overlay structure to allow restarting of calculations. Our original modifications to the code's overlay structure prevented this because of a failure to include some of the code's common blocks in the appropriate subroutines when the new structure was generated. These changes had no effect on analyses previously performed since none of them involved restarts.

A version of the EXTRACT utility program, which creates a completely new input deck, or portions thereof, from a restart file, was developed for TRAC-PF1/MOD1 at Sandia during the latter part of the quarter. Debugging of that program should be completed in April, and it will then be provided to the TRAC developers for further distribution. The utility was developed in the form of a set of updates to the TRAC source file to help alleviate any conversion problems to other machines. Although the updates produce a

stand-alone utility program, which is executed independently of TRAC itself, a few actual TRAC updates were also developed to write the user-entered component IC to the TRAC dump file for use by the EXTRACT utility.

The Sandia-developed TRAC plot program was modified this quarter so that it is no longer necessary to enter component and cell numbers for type 0 (system) or type 9 (control block and signal variables) edit quantities. The positioning of symbols on plots was also changed to prevent overlapping of the symbols.

2.2 B&W OTSG LOFW Tests

Steady state test 28 and its associated loss-of-feedwater (LOFW) transient test 29 in the Babcock & Wilcox (B&W) 19-tube once-through steam generator (OTSG) test facility [4] has been analyzed as part of the TRAC-PF1/MOD1 independent assessment program at Sandia National Laboratories. This test was also analyzed as part of our RELAP5/MOD1 independent assessment project. [5] The primary objectives of the B&W steam generator tests were to determine steady state operating conditions such as mass inventory, temperatures, and pressure drops, and to determine the secondary steam flow during a LOFW transient. The TRAC model we developed for the OTSG was described in the last quarterly [2], as were preliminary steady state results for test 28. Steady state and transient calculations were both completed this quarter. Because of the proprietary nature of the B&W test data [4], only a brief qualitative description of the TRAC calculations will be presented. A topical report describing the details of the facility and the TRAC calculations is in progress. [3]

A major interest in this assessment was the calculation of the two-phase pressure losses associated with turbulent effects at the tube support plates on the secondary side. We have been attempting to develop guidelines on how to correctly model the associated wall friction and form losses, possibly through adjustment of the hydraulic diameter and flow areas, and through addition of user-input form loss coefficients at these cell edges. In our first calculations [2], the hydraulic diameter at the tube support plates was simply set equal to the secondary side tube bundle hydraulic diameter and no additional form losses were included. We also input the minimum tube-to-tube spacing for the heated equivalent diameter used for heat transfer on the outside tube surface, as was done in the RELAP5 model; previous experience with both RELAP5 and TRAC have indicated that this is a more representative value for flow through a bank of tubes than using the hydraulic diameter of the adjacent cell.

Two methods of modelling the support plates (orifices) are available in TRAC. The first method is the automatic form loss option; the second method involves the use of user-input form loss coefficients (K factors). The TRAC input model for the calculations this quarter was changed from that reported in the previous quarterly; in order to use the automatic form loss option in TRAC, we found that two mesh cells per tube support plate were required on the secondary side. Therefore, the TRAC input model now consists of 85 mesh cells (with 35 on the primary side and 50 on the secondary side). The new TRAC noding diagram is shown in Figure 2.2.1.

Using the automatic form loss option in TRAC, as described in the TRAC reference manual, resulted in 40% underprediction of the boiler differential pressure. However, if the flow area of the vena contracta (instead of the actual area of the tube support plates) was used, the predicted boiler Δp agreed extremely well with experimental data. The reason for this is that the pressure loss associated with flow through an orifice is a result of the fluid expansion from the vena contracta to the downstream area and not from the orifice itself. TRAC neglects this effect. An empirical correlation (taken from the RELAP5/MOD1 code), based on the orifice geometry, was used to calculate the vena contract area. We also modified the hydraulic diameter used for wall friction calculations at the support plates. Both of these modelling changes were based on guidelines developed during our PKL assessment analyses, as discussed in the next section.

The second method of modelling the tube support plates, user-input K factors, also resulted in very good agreement with experimental data. The K factors were determined using the Crane handbook [6], based on the geometry of the support plates. The other global parameters measured during the experiment (primary side ΔT, secondary side exit temperature and secondary side inventory) were calculated well by TRAC with both support plate models. However, the elevation at which dryout (end of nucleate boiling) occurs in the boiler predicted by TRAC was approximately 30% too low. This did not significantly influence the total primary-to-secondary heat transfer rate, but indicates that TRAC's dryout criterion is inadequate for this experiment.

Our previous assessment calculations with RELAP5/MOD1 [5] for the same tests indicated that RELAP5 also underpredicted the dryout elevation. In addition, RELAP5 also greatly underpredicted the critical heat flux (CHF). We found that a much better prediction of CHF could be achieved with RELAP5 by changing the CHF correlation from a modified Zuber to a combined modified Zuber/Biasi correlation. Modified Zuber was used for mass fluxes less than 100 kg/m**2-s, Biasi was used for mass fluxes greater than 300 kg/m**2-s and linear interpolation was used in between. (The

mass flux was approximately 200 kg/m**2-s for these tests.) TRAC currently uses the Biasi CHF correlation only. Also, the dryout criteria in RELAP5 was changed to force dryout at a quality equal to the upper limit of the experimentally determined range. This modified version of RELAP5/MOD1 accurately predicted the elevation of dryout as measured in the experiment. Later calculations with RELAP5/MOD1.5 showed that code predicts the experimental behavior correctly without any modifications.

The LOFW transient calculation demonstrated that excellent agreement with experimental data could be achieved using both methods of modelling the tube support plates. We found that, as long as the correct steady state conditions were achieved, there was no problem with predicting the transient response. This was true for both TRAC and RELAP5.

To supplement the straightforward assessment of TRAC against data, we also performed a noding study, because most plant analyses would not be able to use a similar fine nodalization due to computer cost and space considerations. This study indicated that good agreement with experimental data could be achieved using 51 mesh cells, but that using 33 mesh cell produced visibly less satisfactory results. The total primary-to-secondary heat transfer rate prediction was good using all three models; however, for plant transient simulations in which the secondary side response is of major interest, a coarse node model may not be adequate. The coarse node calculation did run approximately two times faster (both steady state and transient) than the base, or detailed, model calculation, which contained 2.6 times as many cells.

2.3 PKL Natural Circulation Tests

The Primarkreislaufe (PKL) test facility [7], located at Erlangen, West Germany, is a 1/134-scale three-loop model of a four-loop PWR. All elevations correspond to a full-scale system, so that gravitational terms are correctly simulated. Core power is provided by 340 electrically-heated rods. The ID1 series of tests [8] was designed to study the natural circulation modes occurring during small break situations in which the primary system was slowly losing inventory. In a continuous operational mode, data for twelve different inventories was recorded, with the test notations of ID1-4 to ID1-15. These data points covered the entire range of potential system response from subcooled natural circulation to reflux cooling.

The TRAC nodalization we developed for the PKL facility was described in the last quarterly [2], as were preliminary results for the basecase single-phase natural circulation test ID1-4. In

that preliminary calculation, we found that the single-phase natural circulation rate predicted (5.35 kg/s) was substantially higher than measured (4.55 kg/s); increasing the code hardwired wall roughness by a factor of eight to a value more representative of that published by PKL only reduced the TRAC predicted flow rate to 5.22 kg/s. These results suggested that we needed to develop a much better understanding of how to geometrically model a facility with respect to piping area changes and wall friction losses with the TRAC code.

This test series had been previously analyzed during our RELAP5/MOD1 independent assessment project. [9] The results showed that RELAP5 did exceptionally well in the prediction of single-phase natural circulation rates for these same PKL tests, as well as for the Semiscale NC series of tests [10], using simple geometric modelling techniques. Therefore, we decided to study the detailed models for area changes used by each of the two codes and try to come up with a set of consistent modelling guidelines to be used for our TRAC analyses.

On the surface, at least, there are substantial differences between RELAP5 and TRAC in their respective treatments of piping area changes and frictional losses. Further, there are no user guidelines for TRAC in this area except a caution in the code documentation about using the automatic form loss calculation option. However, the results of our study of the detailed models indicates that, in most cases, the modelling guidelines we developed and used in our RELAP5 assessment analyses could be converted for use in our TRAC analyses, using the automatic form loss models already present in TRAC. In some cases, exact agreement with RELAP5 formulations could not be obtained, but the differences were small. There are still some questions regarding the use of the automatic form loss option at two consecutive junctions which we have not been able to fully resolve; we currently recommend that the user avoid such use.

We have investigated three basic cases of piping area changes: (a) an abrupt expansion, (b) an abrupt contraction, and (c) an orifice. Schematic pictures of typical TRAC nodings for each of these cases are given in Figure 2.3.1. Single-phase flow in the pipe is assumed to be from the cells on the left to the cells on the right of the figure in all the following discussion, but the code will properly handle flow in the other direction without modification.

The case of a simple expansion will be discussed first. For this case, the TRAC code description correctly states that the numerics used in the code will yield the appropriate pressure drop without benefit of further form losses, either code-calculated when using the negative NFF option, or user-input. However, the

user should be aware that all of the pressure drop will not be taken at the junction where the expansion is physically represented in the nodalization. Instead, the pressure loss at that junction (J in Figure 2.3.1a) will be larger than expected and the pressure loss at one junction downstream in the flow path (D in Figure 2.3.1a) will be less than expected.

This effect is illustrated in Figure 2.3.2, which shows the form loss coefficients used by both TRAC and RELAP5 for such an expansion. These form losses can be related to a pressure difference, frequently referred to as a dynamic head loss, in standard Bernoulli equation format [6] by the equation

$$H_x = 1/2 \ K_x \ \rho^* v_J^* v_J \qquad (2.3.1)$$

(As indicated, the analyst should always use the velocity at junction J to determine the pressure change associated with any of the K components given in the figure, even for the "NUMERIC-D" curve, since all other effects of the area change have already been taken into account when deriving these curves.)

Several curves of form loss coefficients versus piping area ratio -- the ratio of areas before and after the expansion -- are given in Figure 2.3.2. The TRAC-related curves have the following meanings. "NUMERIC-J" identifies the effective K at junction J resulting solely from the TRAC numerical solution scheme; "NUMERIC-D" identifies the effective K at junction D resulting from the TRAC numerical scheme; "NUMERIC-TOTAL" then identifies the sum of those two numerically-based Ks, even though they are effective at different junctions. The analyst has no direct control over these numerically-based Ks; they are totally determined by the geometric input description.

The "ABRUPT AREA" curve represents the form loss coefficient applied at junction J which is calculated in subroutine FWALL when the negative NFF option is used. If positive NFFs are input, no such additional term is calculated. "TRAC TOTAL" represents the sum of all the above terms.

A curve identified as "RELAP5 TOTAL" is also shown in Figure 2.3.2. It represents the total effective form loss coefficient which would be calculated by RELAP5 for that area change. In RELAP5, all the pressure change would occur at junction J and it is all the result of using the abrupt area change model, since the RELAP5 numerics do not naturally produce dynamic head losses due to area changes, as the TRAC ones do.

A cursory investigation of the curves for the total effective Ks for abrupt expansions in RELAP5 and TRAC indicates that they are always the same when both codes are flagged to use their

respective abrupt area change models, but the curves are, in fact, slightly different for area ratios between 0.9 and 1.0 because the TRAC abrupt area model produces a slightly negative K in that range. Since the TRAC abrupt area change model provides a zero or negligible contribution for this particular case, the analyst may be tempted to use the positive NFF option for an expansion. However, this will create difficulties during flow reversals when the same area change becomes a contraction, as will be discussed next.

For an abrupt contraction, shown schematically in Figure 2.3.1b, the TRAC numerics do not automatically produce the correct form loss. That fact is illustrated in Figure 2.3.3, which shows that all the TRAC numeric form loss for a contraction is actually taken at junction J and is considerably higher than that which would be predicted by RELAP5 for area ratios less than 0.5. If the negative NFF option is used in TRAC, a negative component is calculated by the abrupt area change model in FWALL which makes the total TRAC and RELAP5 curves much more similar over the entire range of area ratios, although not identical. As mentioned above, we therefore recommend that the negative NFF option be used for such contractions/expansions.

For a simple orifice (such as shown in Figure 2.3.1c), the various K components are shown in Figure 2.3.4. In this case, it would seem that there is no simple modelling guideline for TRAC which would yield pressure drop characteristics even remotely similar to those obtained with the RELAP5 area change model. However, closer inspection reveals the fact that TRAC and RELAP5 can be made to yield identical form loss coefficients for an orifice if the TRAC negative NFF option is used and the vena contracta area for the orifice is input to TRAC as the junction J area, instead of the physical orifice area. The vena contracta area is calculated in subroutine HLOSS of RELAP5 via the simple empirical formula

$$A_C = A_T [0.62 + 0.38 (A_T/A_P)**3]$$

where A_C is the vena contracta area, A_T is the physical or "throat" area of the orifice, and A_P is the open area of the pipe containing the orifice. We recommend that this formula be used to determine the flow area to be input to TRAC at junction J in Figure 3.2.1c.

Another important factor in determining the single-phase natural circulation flow rate is the frictional wall resistance of the piping. In the TRAC code, the frictional pressure loss is based on hydraulic diameters input for the junctions between the fluid cells, since the velocities are calculated by the code at that point. In essence, the hydraulic diameter input at a given

11

junction is used to calculate the wall friction corresponding to half of the cell upstream of the junction and half of the cell downstream of the junction. In straight piping, that formulation presents no problem because the average fluid velocity over the length of the cell actually containing the piping walls is basically constant. When an abrupt area change is encountered, however, the hydraulic diameter input must represent the walls for two different-sized pipes for an expansion/contraction and also must reflect the fact that the fluid velocity at the junction may be larger than that seen by the piping walls, particularly at an abrupt orifice.

To more properly reflect the frictional loss corresponding to piping walls near abrupt area changes, we recommend using the following formula to determine the hydraulic diameter input to TRAC at area changes such as those shown in Figure 2.3.1:

$$HD_J = \frac{(\Delta X_j + \Delta X_{j+i})}{\left[\left(\frac{A_J}{A_j}\right)^2 \frac{\Delta X_j}{HD_j} + \left(\frac{A_J}{A_{j+1}}\right)^2 \frac{\Delta X_{j+1}}{HD_{j+1}}\right]} \qquad (2.3.2)$$

In this formula, ΔX represents a cell length, A is either a cell or a junction flow area, and HD is a hydraulic diameter. The quantities with lower case subscripts j and j+1 represent "volume-centered" or "cell-centered" quantities, whereas those with the capital subscript J are for the junction between cells j and j+1. The cell-centered areas and hydraulic diameters used by the analyst to calculate HD_J should take into account any effect of "lumping" of flow paths, such as combining multiple intact loops into one or combining all the steam generator tubes into one flow path. Equation 2.3.2 is applicable for all three area change cases depicted in Fig. 2.3.1.

After the above-described modelling guidelines were used to modify the TRAC input description for test PKL ID1-4, the steady state single-phase mass flow was predicted to be exactly the same as the measured value, 4.55 kg/s. The fluid temperatures around the loop were all a few degrees higher than measured, as shown in Figure 2.3.5, but generally within the experimental uncertainty of ± 3 K. (RELAP5 also predicted loop temperatures a few degrees higher than the data.)

Our TRAC ID1-4 calculation was run for 5000 s of problem time to ensure stable conditions. The achievement of steady state conditions is illustrated in Figure 2.3.6, which gives calculated hot leg liquid temperatures at several points along the hot leg, and Figure 2.3.7, which shows the mass flow at several points in the primary system, as a function of time into the calculation.

Some jitter is seen in both the mass flows and the fluid tempera-
tures, but the system is calculated to be reasonably stable after
about 2500 s. The calculation was also restarted at 5000 s with
the maximum allowed time step reduced by a factor of 4 (from 1 s
to 250 ms) and run for another 800 s. The smaller time step
helped smooth the results, but did not eliminate the jitter
entirely.

After satisfactory agreement was obtained for test ID1-4 and
we were convinced that our basic TRAC geometric model for PKL was
satisfactory, work was initiated on the analysis of tests ID1-8
through ID1-15, the two-phase natural circulation tests. The
initial conditions were modified from the ID1-4 input deck to
reflect the lower primary and secondary pressures for those
two-phase tests. A huge number of signal variables and control
blocks were also added to the input deck so that we could monitor
the system inventory.

Attempts were first made to drain the system to the 95%
inventory using the new PID controller in TRAC, but the results
were not satisfactory because we could not easily determine an
appropriate set of time constants to be used. We then decided to
control the drain valve with a more straightforward controller
which adjusted the valve area linearly, depending on the differ-
ence between the current inventory and the desired inventory.
That approach was successful in achieving the correct inventory
over a reasonable period of time in the calculation, but the mass
flow and system pressure and temperature results were consider-
ably different than measured.

Based on a restart printout, we initially suspected that the
calculated results for this first run of ID1-8 might be in error
because the heat slab temperatures in the model were not stabi-
lized at the right value. We then discovered that, in fact, the
printout was wrong because of TRAC coding errors and we corrected
the coding. We have not yet determined the actual reason for the
initial poor disagreement for test ID1-8. It might be because of
incorrect conditions used for our "steady state" before we
started draining the inventory to the 95% level. That will be
studied next quarter.

2.4 Condensation Separate Effects Tests

During the quarter, we began a sequence of calculations
investigating TRAC's ability to model horizontally stratified
cocurrent flow, for comparison with experimental data produced at
Northwestern University. [11] The problem being addressed is that
of flow (at roughly atmospheric pressure) in a rectangular
channel approximately 1.6 m long, 0.3 m wide, and 0.06 m high, as

shown in the upper portion of Figure 2.4.1. Heat transfer at the channel walls is assumed to be negligible. The vapor is super-heated, and variations are performed on inlet flow rates, liquid level, and the amount of subcooling of the liquid (as shown in the test matrix given in the lower portion of Figure 2.4.1). The experiments are very simple, and calculated results should display the effects of mass, momentum, and energy transfer at the interface, as well as those of wall friction.

The TRAC nodalization for these calculations consists of a source for vapor and liquid at the inlet, a 50-cell, 1.25 m flow channel, and an outlet boundary condition. (The maximum flow distance for most experimental data of interest is ~ 1.23 m.) The boundary conditions are constant in time, and TRAC's steady state option was used. In hopes of accelerating the convergence process, linear interpolation was used for those initial conditions which varied significantly along the flow path. The first calculations we tried were for the conditions of test 253.

In our initial calculations, TRAC was allowed to choose a time step as large as 1 s, and those preliminary results suggest that the time step selection algorithm is inadequate for ini-tialization in situations with two-phase flow dominating. This was evidenced by repeated sequences in which the time step grew at the maximum rate, and was then sharply reduced; the results showed no prospect of reaching a steady state, at least in a reasonable amount of computer time. Figure 2.4.2 presents typical histories for the time step and the liquid velocity halfway down the flow channel.

Successive factor-of-two reductions in the maximum allowed time step showed that the steady state convergence convergence criteria would be met in ~ 60 s of problem time, at a maximum time step of 0.25 s. A further time step reduction resulted in convergence in 35 to 40 s of computed time; however, the state at convergence was not the same as that attained with the larger time step (Figure 2.4.3). Calculations with maximum time steps of 0.125 s and 0.0625 s did yield virtually identical results, so the larger of these two time steps was chosen for our later "base-case" analyses. As a part of this study, the steady state convergence criteria were modified so that the quantities checked are normalized rates-of-change of the fluxes of mass, momentum, and total energy for each phase. This alteration had only a small effect on the course of the calculations; predictably, conver-gence to a steady state required slightly more computer time.

14

The data presented for the experiments consist mainly of liquid film thicknesses, vapor mass flows, and pressure increases at 5 stations along the flow path. It therefore seemed that the TRAC model should be able to use either a pressure ("BREAK") or velocity ("FILL") boundary condition for the outlet. Figure 2.4.4 compares experimental and calculated pressure difference profiles using both velocity and pressure boundary conditions at the outlet. The calculated result with the pressure boundary condition is only numerically wrong, but the velocity boundary condition yields a qualitatively incorrect pressure profile. In the case of the vapor mass flux, a similar situation exists, with the roles of the calculated results reversed; as shown in Figure 2.4.5, the pressure boundary condition causes negative calculated flow in the downstream one-quarter of the channel. Both the pressure and the mass flow comparisons are consistent with the hypothesis that TRAC overpredicts the amount of condensation, and suggest that the phase-change model should be examined.

TRAC computes the phase-change rate by equating the energy transferred from each phase to the interface with the enthalpy jump required for the phase change. Thus, the interfacial heat transfer coefficients and the effective areas control the process. For the interface-to-liquid contribution, the term of interest is proportional to the product of liquid velocity, density, specific heat, and the interface area (i.e., the liquid Stanton number is constant). The vapor-to-interface contribution is more complicated; however the area term used does not appear to depend on the stratified interface area.

We are testing a very simple alteration in the model for interfacial heat transfer in completely stratified flow. As viewed from either phase, the interface is considered to be a flat plate; analysis for a boundary layer replaces that for flow in a pipe, and prescribes the Stanton number to be proportional to a product of powers of the Reynolds and Prandtl numbers. (See, for example, Reference 12.) For the liquid term, the effect is one of multiplying the "standard" heat transfer coefficient by a constant, a power of the Prandtl number, and a power of the Reynolds number. The vapor-to-interface and liquid-to-interface terms are identical in form, differing only in the quantities used to evaluate them. The area of the stratified interface thus affects energy transfer for both phases. Because of the boundary layer approach, the characteristic length in the Reynolds number is distance from the inlet, and the mean relative velocity is used. The multiplicative constant and the exponent on the Reynolds number depend on whether the flow is laminar or turbulent, and transition between those regimes is accomplished by a cubic in the velocity. Figure 2.4.6 compares the standard and modified interfacial heat transfer coefficients for conditions typical of these analyses. Although we expect frictional effects

15

to be much less important in these calculations, we have included
a similar treatment based on Reynolds' analogy for wall friction,
for the sake of consistency. In this case, of course, the mean
velocity of each phase is used. No alterations to the interfacial
friction description were made.

We performed calculations using both standard and modified
models, for two sets of inlet conditions -- Tests 253 and 259 in
Figure 2.4.1. The major difference in the conditions is that one
set has an inlet vapor mass flux about 2.5 times that in the
other. Direct comparison with the data is somewhat ambiguous,
because of the differences between the rectangular test channel
and TRAC's circular pipe geometry. However, on the basis of
pressure differences and mass flows (given in Figures 2.4.7 and
2.4.8), the results using the modified code are closer to the
data than those obtained with the standard models for the lower
flow case. Countercurrent flow does not occur using the modifi-
cation, and the two outlet boundary conditions give more similar
results. With the higher flow, neither method is clearly
superior; however, TRAC obviously gives (with or without modifi-
cation) a correct qualitative prediction of the effect of
increasing the inlet vapor flow. As expected, the modified
version of the code yielded lower interfacial heat transfer and
phase change rates than those given by the standard model, as
shown in Figures 2.4.9 and 2.4.10.

The approximations to the stratified flow field we used to
develop the modified treatment are very crude, and can probably
be refined quite easily to include an analysis of the boundary
layer at the interface. We will investigate this question in the
near future. We will also consider test points with other inlet
conditions, to assure that TRAC correctly predicts the effects of
varying those conditions.

The reader should be aware that a large part of this separate
effects assessment analysis so far has been devoted to providing
"signal variable" definitions for analyzing the output, and pro-
cessing the graphics file content so that convenient comparisons
can be made with experimental data. This work also exposed some
relatively minor code and documentation errors, which have been
discussed with the code developers.

2.5 NEPTUNUS Pressurizer Test

The NEPTUNUS pressurizer test facility, located at Delft
University of Technology, consists of a 2.5 m high by 0.8 m
diameter test vessel with a 0.084 m diameter surge line and a
0.027 m diameter spray line. Heater elements with a total power
of 17 kW were installed in the facility to offset environmental
heat losses.

Test Y05 from the NEPTUNUS facility is being analyzed using TRAC-PF1/MOD1. The input for this model was taken from a paper by H. A. Bloemen in which an analysis of this test using RELAP5/MOD1 was discussed [13]. Test Y05 consisted of four insurges and outsurges combined with four cycles of spray. The measured surge line and spray flows are shown in Figure 2.5.1 and illustrate that the test was initiated from an insurge followed shortly by the initiation of spray flow. The temperature of the surge line flow was constant at 548 K and the spray temperature varied from 594 K to 500 K. In addition to the flows and temperatures in the surge and spray lines, the pressure and three fluid temperatures at one elevation in the test vessel were measured. This test was analyzed with TRAC-PF1 because the capability of computer codes used in safety analyses to calculate correct pressurizer response is an important concern of the NRC.

The test facility is a relatively simple system and the nod-ing diagram illustrating the TRAC-PF1 model used for the analysis is shown in Figure 2.5.2. The model has three components, a pressurizer and two fills. One of the fills simulates the surge line and the other the spray line. Two nodings were used for the pressurizer: 13 cells and four cells.

The calculated (13-cell model) and measured pressures at the elevation corresponding to cell 9 of the 13-cell model are com-pared in Figure 2.5.3. The pressures initially increase because of the flow in from the surge line. The pressures decrease as a result of the subcooled spray flow and an outsurge from the pres-surizer. The four cycles in the pressures are a result of the four insurges and outsurges. The calculated changes in pressure during both insurges and outsurges are higher than the measured change; however, relatively good agreement in the minimum pressure occur. The calculation of a higher pressure during insurges with spray flow may indicate that the interfacial heat transfer for subcooled water is too low.

Calculated and measured fluid temperatures are compared in Figure 2.5.4. Three measurements of the fluid temperature are shown. Similar to the results from the comparison of the pres-sures, the temperatures increase during insurges and decrease during spray flow and outsurges. During the insurges the calcu-lated and measured fluid temperatures indicated the vapor was superheated, with the calculated fluid temperature being higher than measured.

To determine the effect of a coarser noding of the pres-surizer on the calculated results, the calculation was repeated with a 4-cell pressurizer. The pressures from the 4-cell and 13-cell models and the measured pressure are compared in Figure 2.5.5. There are some small differences in the maximum pressures

17

during the insurges. The minimum pressure from the 4-cell model was slightly lower than the 13-cell model. This difference appears to be caused by the fluid temperature being lower with the 4-cell model, as shown in Figure 2.5.6. The generally lower temperatures with the 4-cell model are a result of the void fraction being higher at the measurement elevation with the coarser noding.

The calculated liquid temperature in the cell the subcooled spray was injected into, the top cell in the model, could be unphysically low if the time step was not controlled. The calculated liquid, spray, and saturation temperatures are shown in Figure 2.5.7. This calculation was run with a maximum time step of 0.25 s and, after the first few seconds, the code selected the maximum time step for the remainder of the calculation. A comparison of the spray and liquid temperatures shows that a lower liquid temperature was calculated than the source spray during some periods of spray flow. The spray should be the coldest liquid in the system. Reducing the maximum time step to 0.05 s eliminated the low liquid temperatures in the top cell. The calculation of low liquid temperatures in the top of the pressurizer did not affect the calculated pressure, which was nearly identical with both maximum time steps.

In summary, preliminary results from the comparison of pressures and fluid temperatures during insurges and outsurges from a pressurizer, with spray flow, indicate that higher maximum pressures and fluid temperatures are calculated by TRAC-PF1/MOD1 than measured. These results may indicate that the interfacial heat transfer to the liquid during condensation is too low. Additional analysis of these results will be performed next quarter.

2.6 LOBI Large and Intermediate Break Tests

The Loop Blowdown Investigations (LOBI) facility, shown in Figure 2.6.1, is located at Ispra, Italy, and supported by the EURATOM Joint Research Centre. [14] The facility was designed to supply experimental data on simulated LWR primary coolant system response during the initial high pressure blowdown portion of a LOCA. It is a 1/700-scale model of a four-loop 1300 MWe PWR, consisting of two primary coolant loops connected to an electrically-heated reactor pressure vessel model, in which 64 rods provide a peak power of 5.3 MW. While both loops contain a fully active circulation pump and steam generator, the intact loop has three times the water volume and mass flow of the broken loop.

The two LOBI tests in our assessment matrix are Al-04R, a 200% cold leg break scenario previously analyzed as part of our RELAP5/MOD1 assessment program [15], and B-R1M, a 25% cold leg break which is a scaled counterpart to Semiscale intermediate break test S-IB-3 (also in our TRAC-PF1/MOD1 assessment matrix). We chose to analyze Al-04R first, since much of the background work had already been done during our RELAP5 analyses.

The steady state and transient TRAC-PF1/MOD1 nodalizations we have developed for the LOBI facility are shown in Figures 2.6.2 and 2.6.3, respectively. Both loops are modelled, with the triple-capacity intact loop shown on the left, the single broken loop on the right and the vessel in the middle. The steady state model contains 37 components, with a total of 167 1-D cells and 78 cells in the 3-D vessel; the transient model contains 40 components with a total of 173 1-D cells. A 3-D VESSEL is used rather than a 1-D CORE component because of the significant core rod heat in the upper plenum; this could not be modelled explicitly in the TEE component that would needed to hook the hot legs to the vessel. Most of the 1-D cells (43 each) are in the atypical LOBI steam generators, which have separate downcomer and boiler regions for the hot and cold leg sides. The transient nodalization is almost identical to the steady state nodalization, except for a few modifications required for the transient, such as modelling the break valve assemblies, the steam generator isolation, and the pump and core power ramps.

During this quarter, the steady state initialization for test Al-04R was completed. Good agreement between measured [16] and calculated initial conditions was eventually achieved for all major parameters. The TRAC steady state calculation was begun by inputting the RELAP5 initial values, rather than from the usual cold no-flow conditions, saving significant computer time. As in our earlier RELAP5 calculations, we found that using the minimum tube-to-tube spacing as the heated equivalent diameter on the outside of the U-tubes (rather than the usual hydraulic diameter) was required to allow simultaneous matching of the primary side cold leg temperature and the secondary side pressure.

The major problem encountered during the steady state initialization was matching the individual loop flows and pump speeds simultaneously, an indication of how well local pressure drops are modelled. Two main changes were required. Loss coefficients associated with tees that were user-input in our RELAP5 model were removed in the TRAC model on the assumption that the TEE component in TRAC would correctly account for the relevant pressure drops. Also, the hydraulic diameters used in calculating the wall friction (which are cell-edge quantities in

19

TRAC rather than cell-center variables as in RELAP) were adjusted, based on the guidelines developed during our PKL analyses, at junctions between two different-area cells. This adjustment was particularly important for the junctions connecting the steam generator plena to the loop piping and to the U-tubes.

Transient calculations for Al-04R will begin next quarter, as well as work on the intermediate break test B-R1M.

2.7 Semiscale Tests

The Semiscale Mod-2A test facility, shown in Figure 2.7.1, is located at the Idaho National Engineering Laboratory and supported by the NRC. This scaled integral facility is used to investigate the thermal and hydraulic phenomena accompanying various hypothesized loss-of-coolant accidents and operational transients in a PWR system. It is a 2/3411-scale model of a four-loop PWR, consisting of two primary coolant loops and an external downcomer connected to an electrically-heated reactor pressure vessel model, in which 25 rods provide a peak power of 2.0 MW. While both loops contain a fully active circulation pump and steam generator, the intact loop has three times the water volume and mass flow of the broken loop.

Of the three Semiscale Mod-2A tests in our TRAC-PF1/MOD1 assessment matrix, we chose to start with the intermediate break test S-IB-3. This test was designed to duplicate as closely as possible the LOBI B-R1M test, which is also in our assessment matrix. The LOBI B-R1M test was a 25% break in the LOBI facility which, when area-to-volume scaled to the Semiscale facility, resulted in a 21.7% break test in the Semiscale facility; both tests simulate cold leg break LOCAs.

The TRAC-PF1/MOD1 nodalization we have developed for the Semiscale Mod-2A facility is shown in Figure 2.7.2. Both loops are modelled, with the intact loop shown on the left, the broken loop on the right and the vessel in the middle. The steady state model contains 28 components, with a total of 180 1-D cells and 48 cells in the 3-D vessel. A 3-D VESSEL is used rather than a 1-D CORE component to allow easier and more accurate modelling of the vessel connections and geometry than could be achieved using numerous TEE components. Many of the 1-D cells (45 and 42 for the intact and broken loops, respectively) are in the steam generators.

The few modifications required for the S-IB-3 transient, such as modelling the break valve assemblies, the steam generator isolation, and the pump and core power ramps, will be made next

quarter, after the steady state calculation is completed. The deck will also then be modified by replacing the 3-D VESSEL with a 1-D CORE and a number of TEEs before beginning the scheduled S-SF-3 and S-SF-5 analyses. Those long-duration secondary side break transients will require fast-running decks more than detailed vessel geometry.
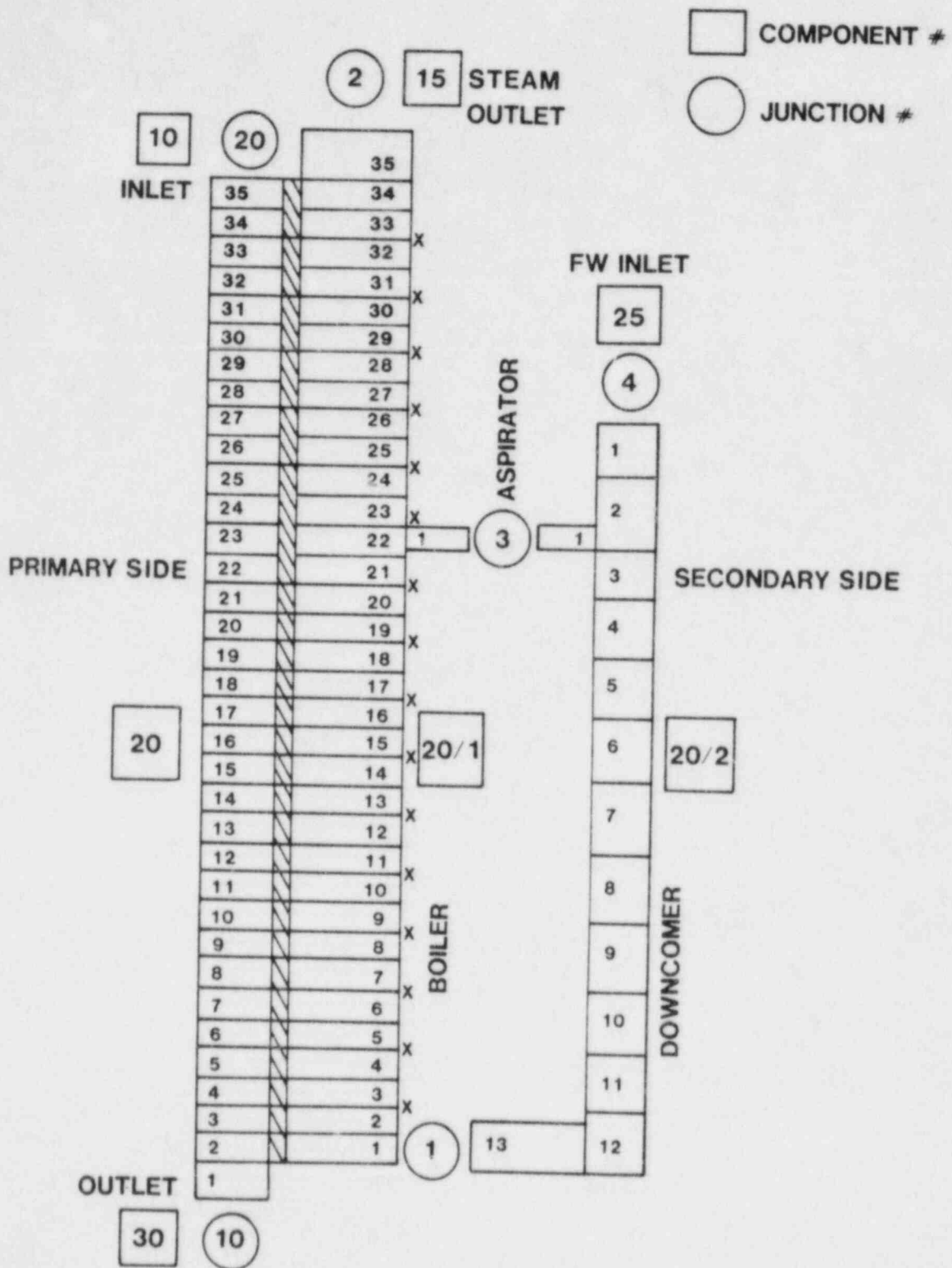
Figure 2.2.1 TRAC-PF1/MOD1 Nodalization for B&W 19-Tube OTSG
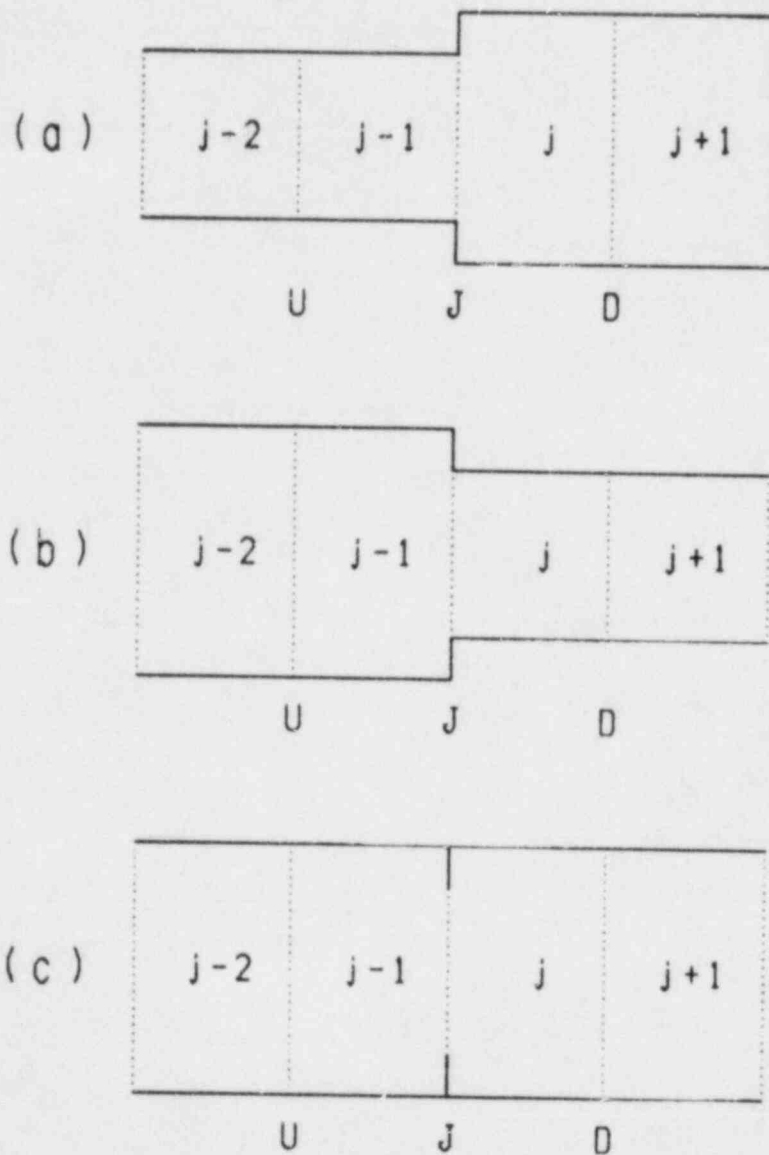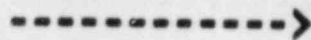
22

ASSUMED FLOW DIRECTION

------------->

(a)   j-2   j-1   j   j+1

      U   J   D

(b)   j-2   j-1   j   j+1

      U   J   D

(c)   j-2   j-1   j   j+1

      U   J   D

Figure 2.3.1   Typical TRAC Noding for an Expansion,
Contraction and Orifice
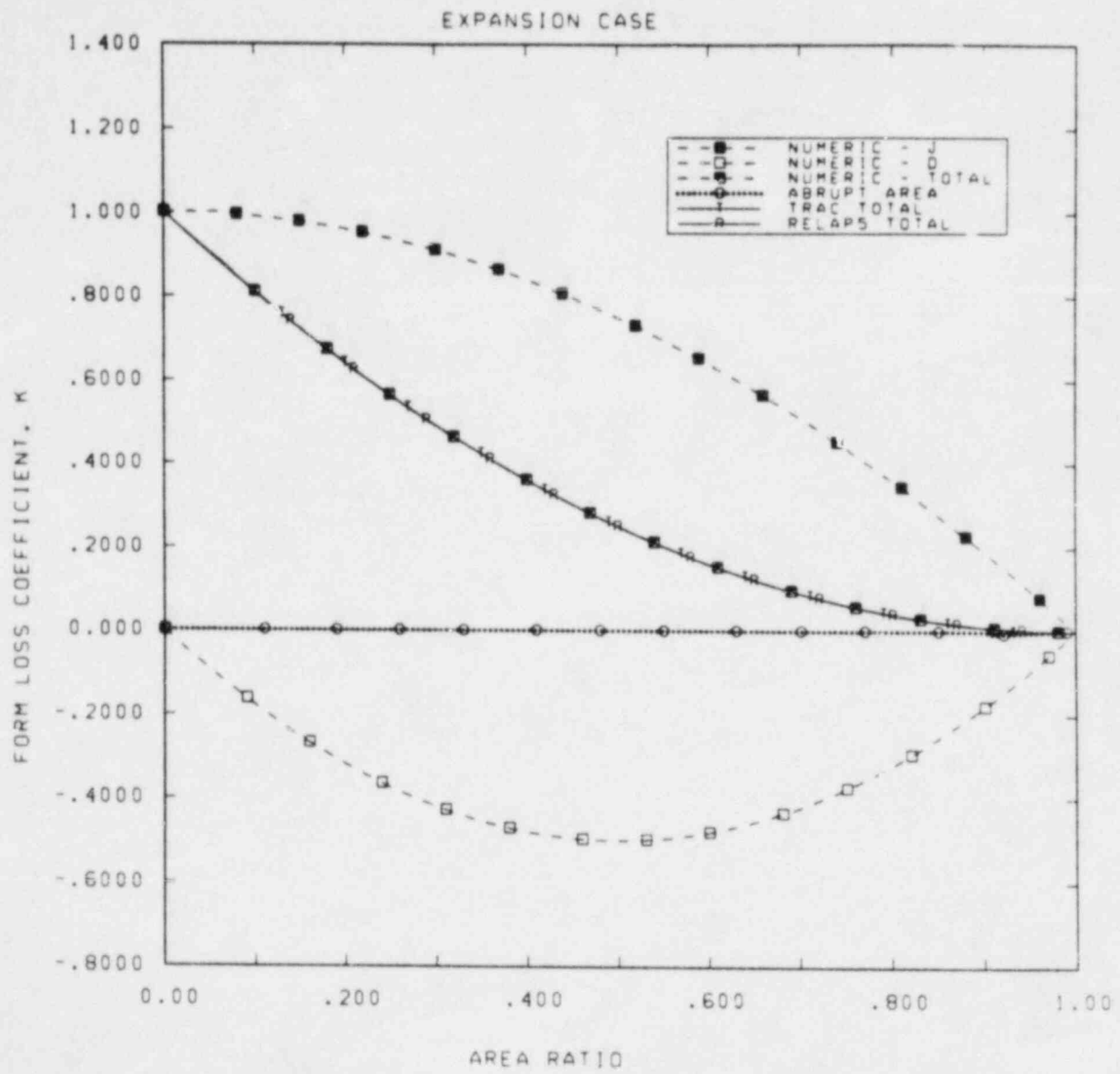
Figure 2.3.2   Form Loss Coefficients vs Area Ratio
for an Expansion

24
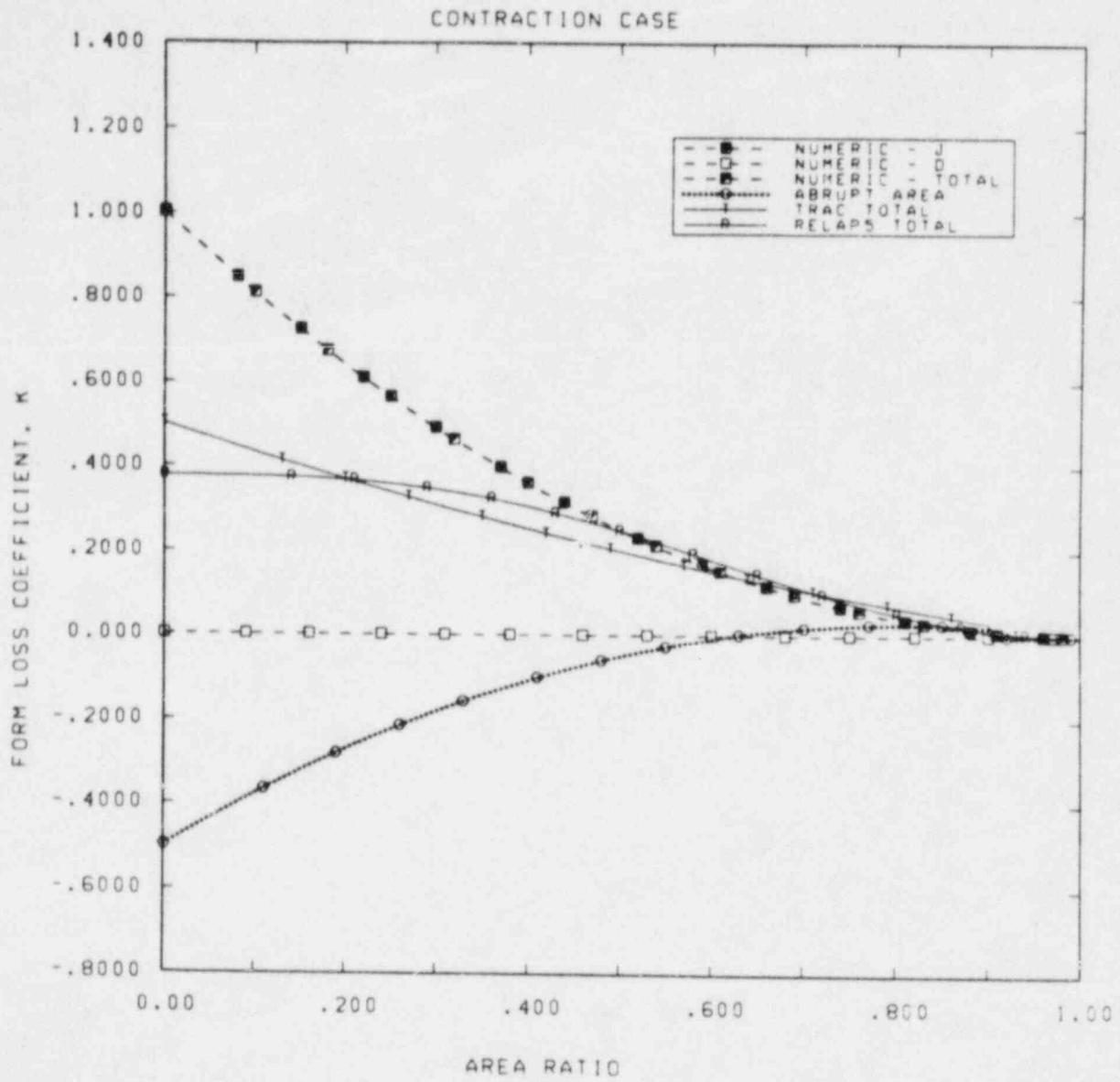
CONTRACTION CASE

Figure 2.3.3 Form Loss Coefficients vs Area Ratio
for a Contraction

25
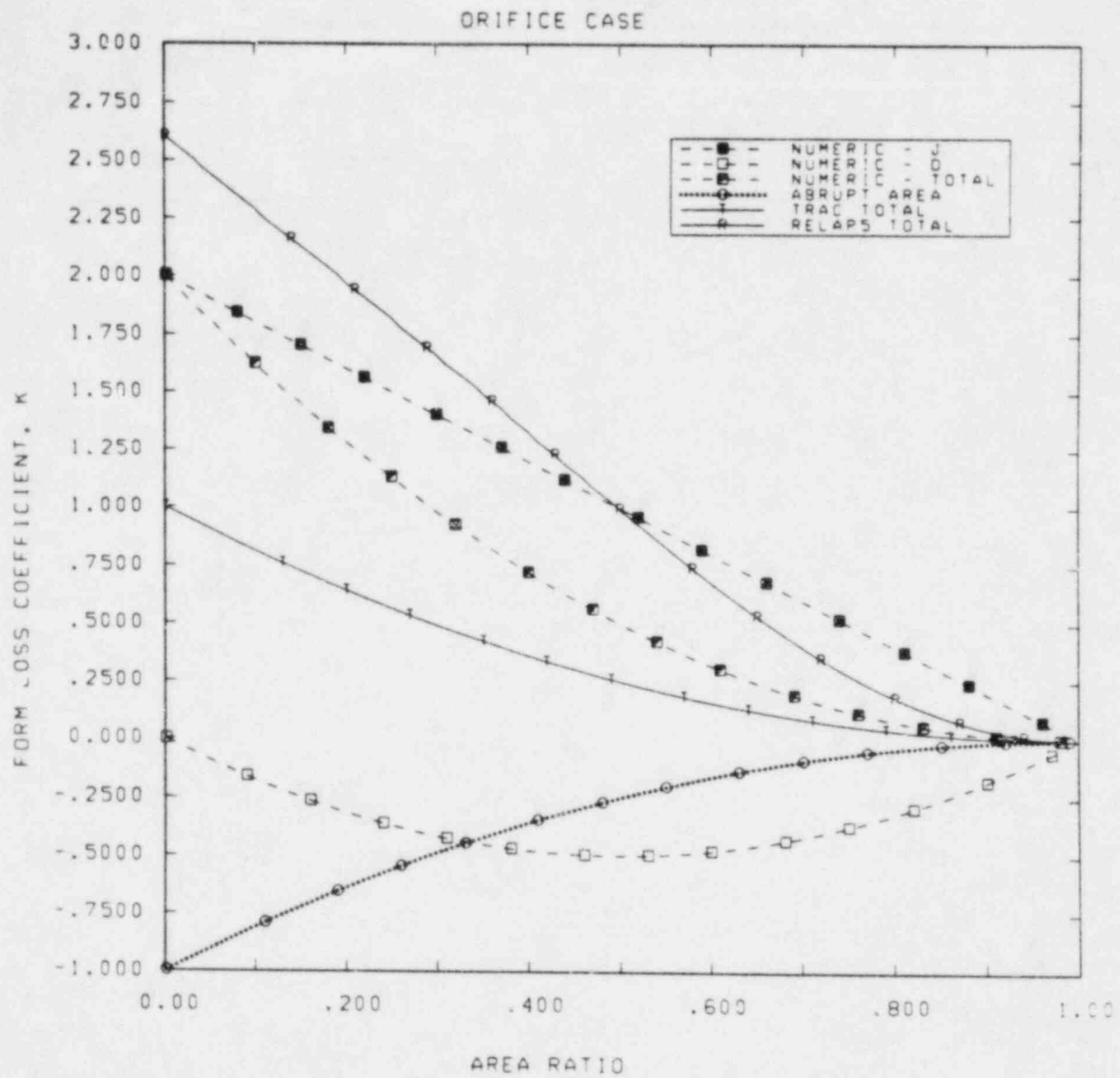
Figure 2.3.4   Form Loss Coefficients vs Area Ratio
for an Orifice

26
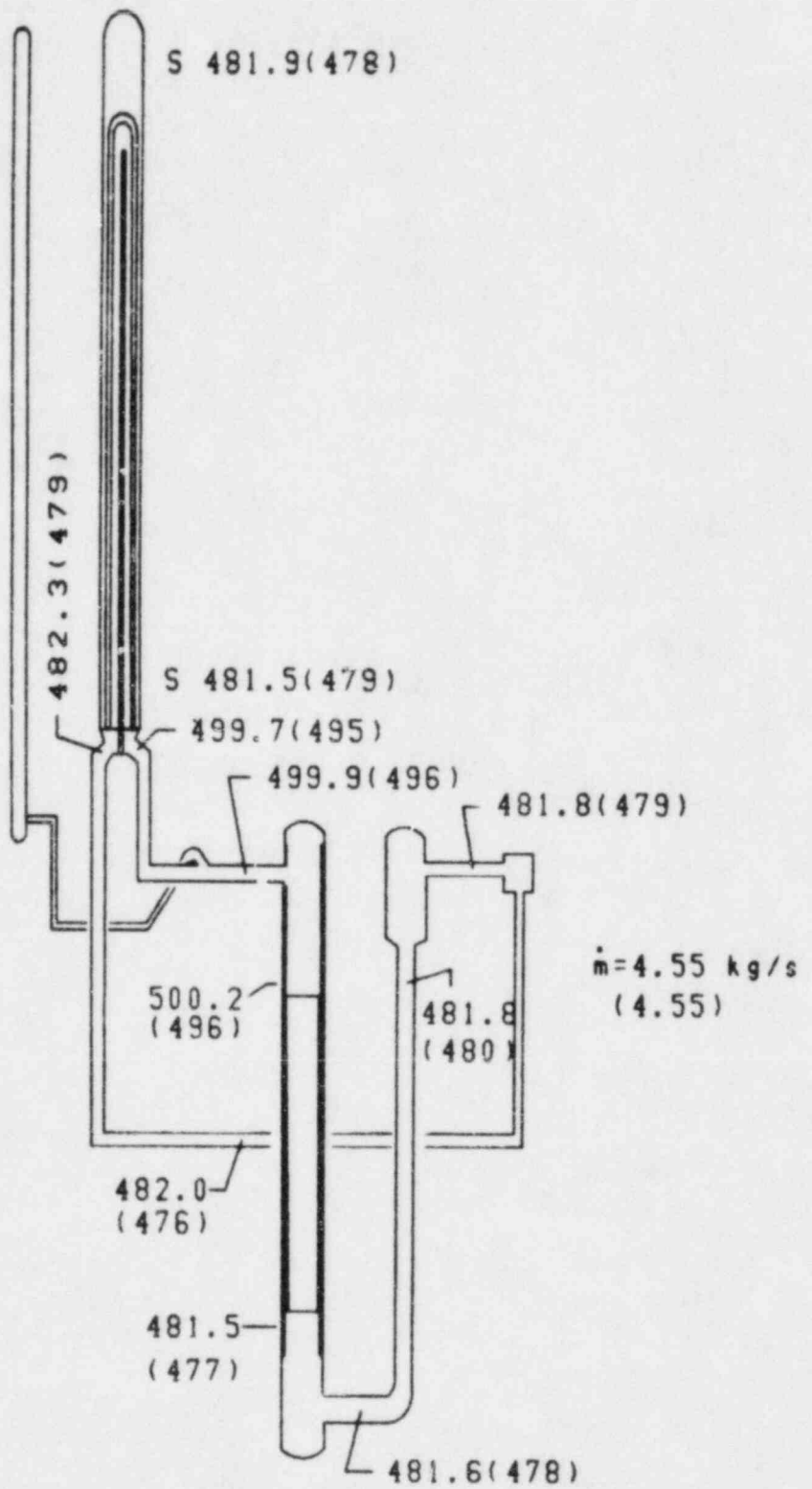
Figure 2.3.5   PKL Test Point ID1-4 Calculated and
                (Measured) Temperatures and Downcomer
                Mass Flows
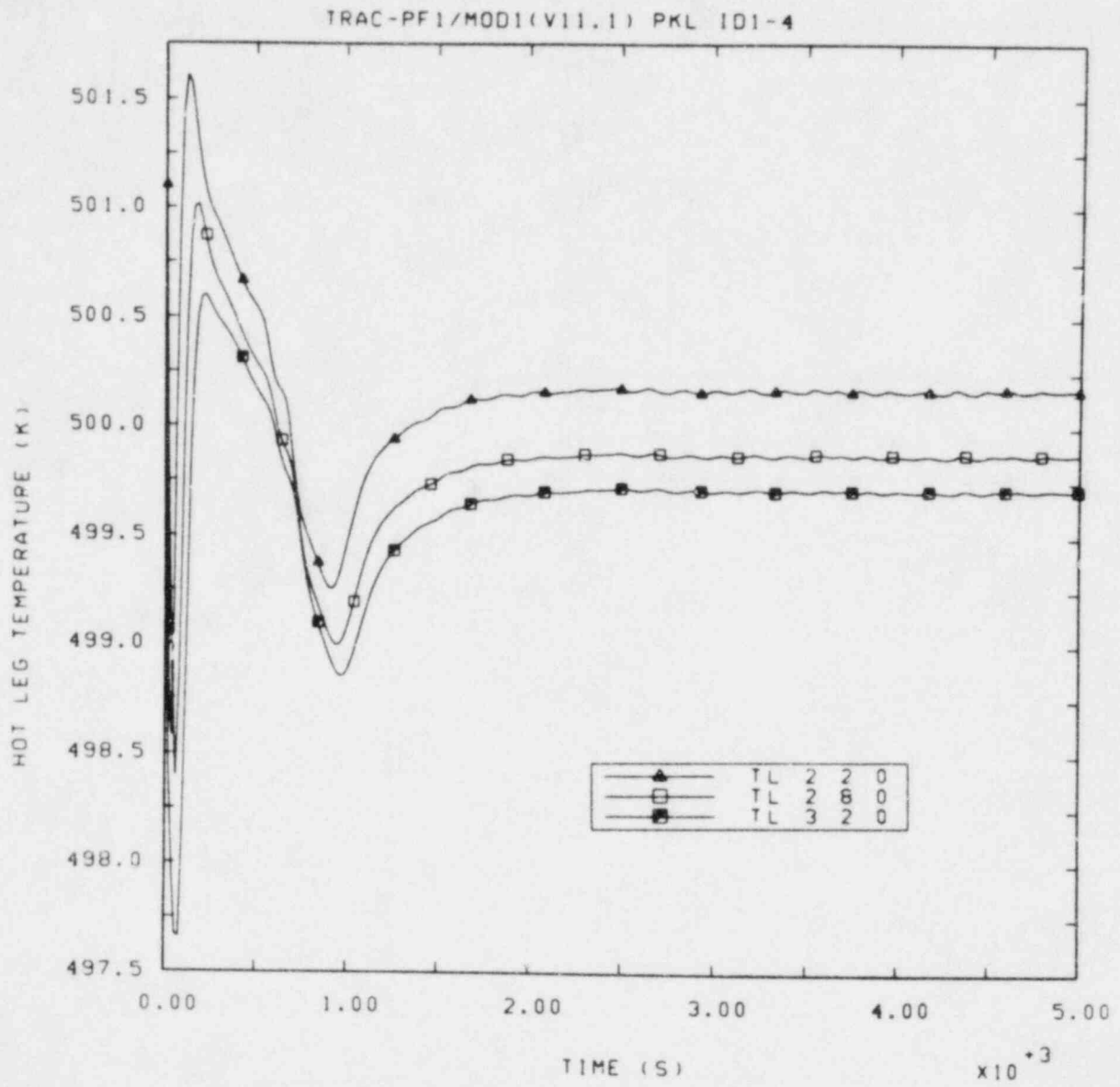
Figure 2.3.6   Calculated Hot Leg Liquid Temperatures
vs Time for PKL ID1-4
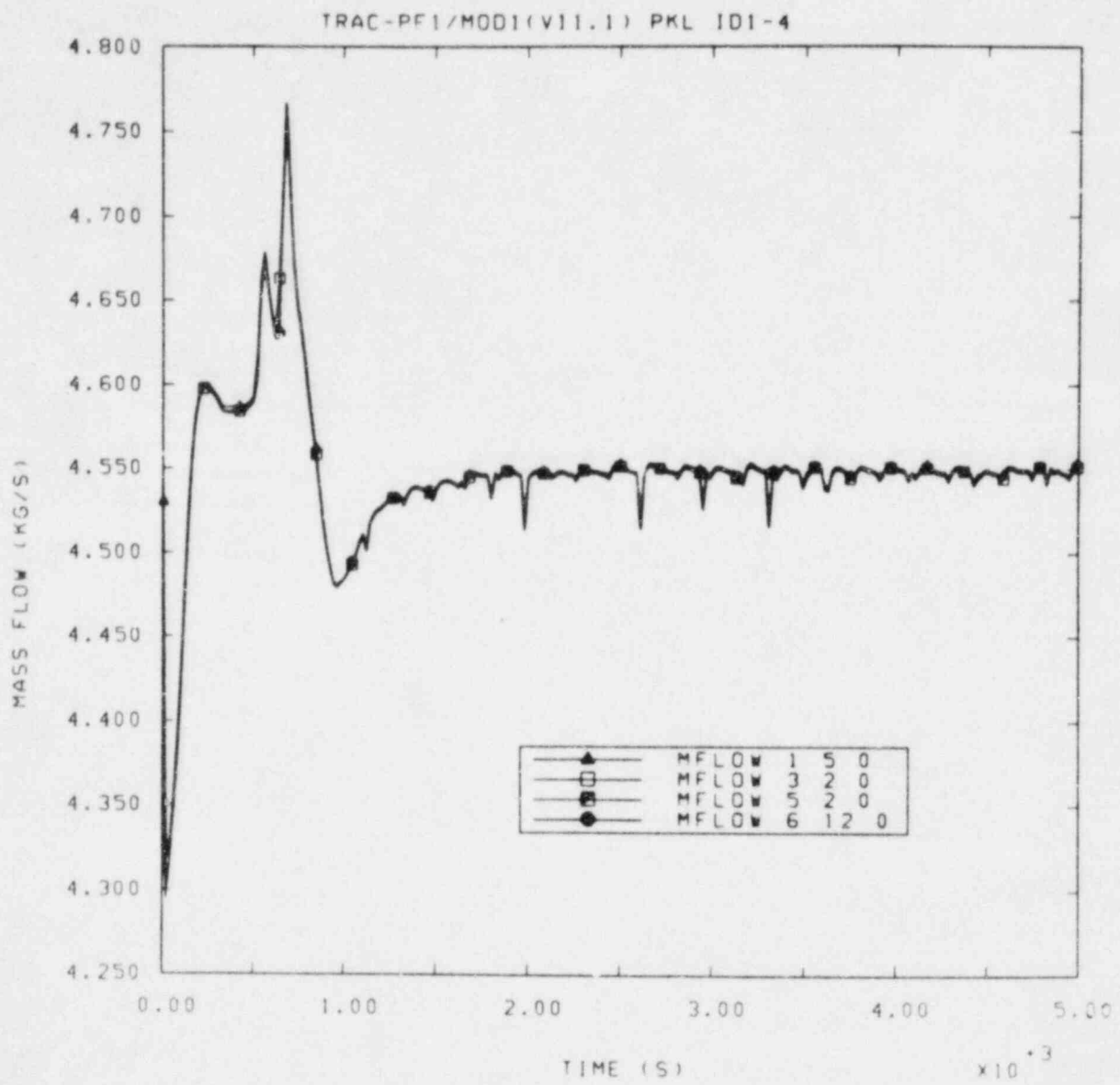
Figure 2.3.7   Calculated Loop Mass Flows vs Time
for PKL ID1-4
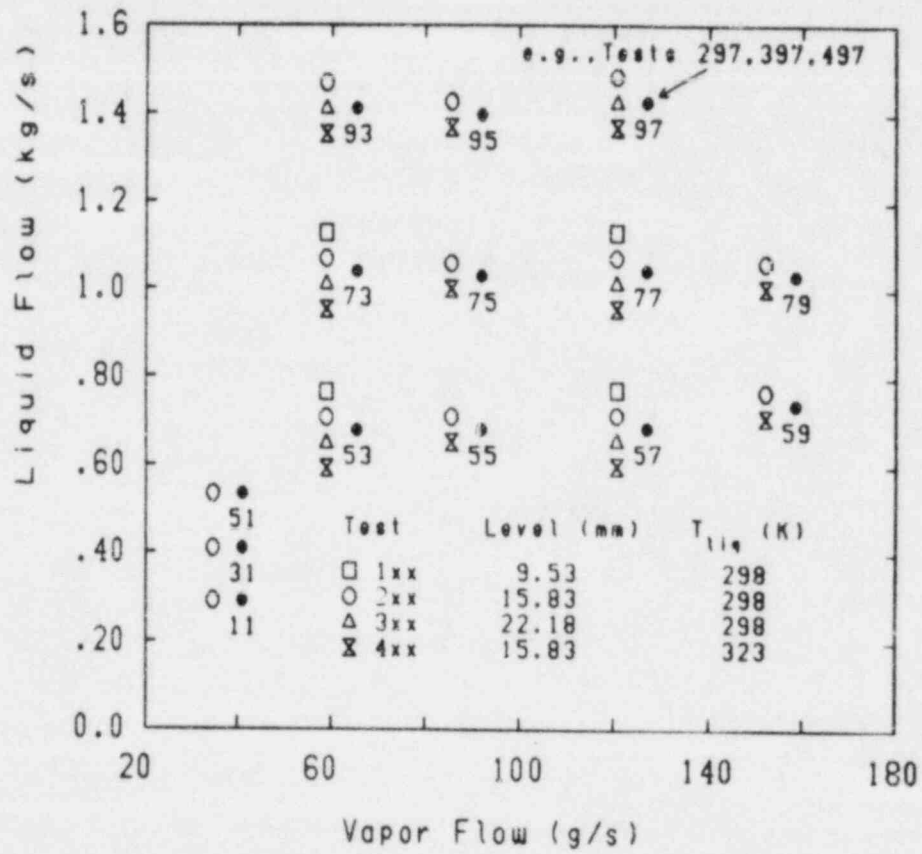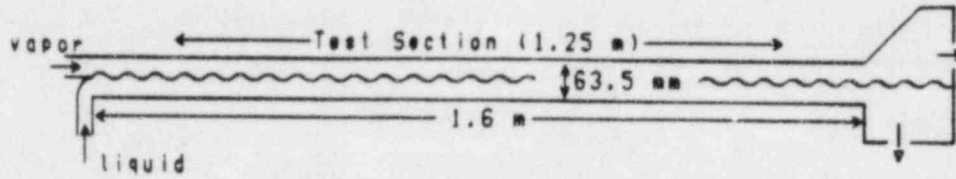
Figure 2.4.1   Test Configuration and Nominal Inlet
Conditions for Stratified Flow Experiments
(after NUREG/CR-2289)
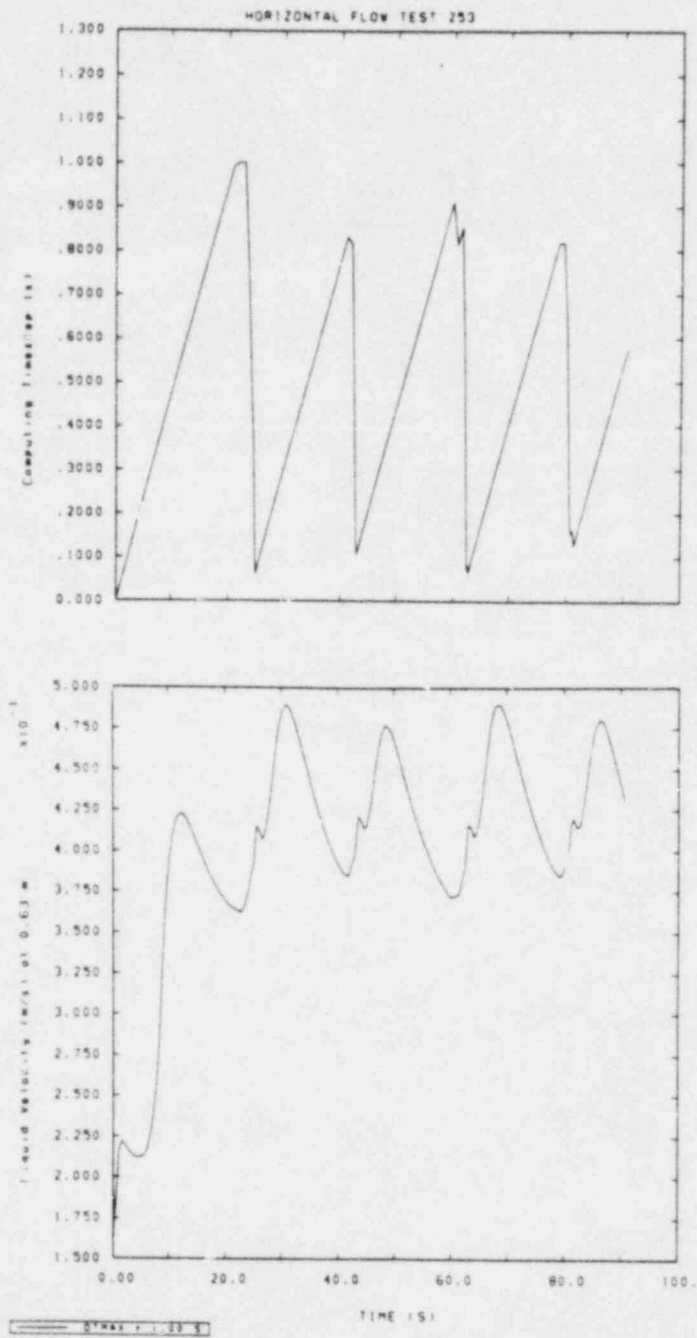
Figure 2.4.2   Results from Steady State Attempt
                using a Maximum Timestep of 1 s:
                Timestep (above) and Liquid Velocity

31
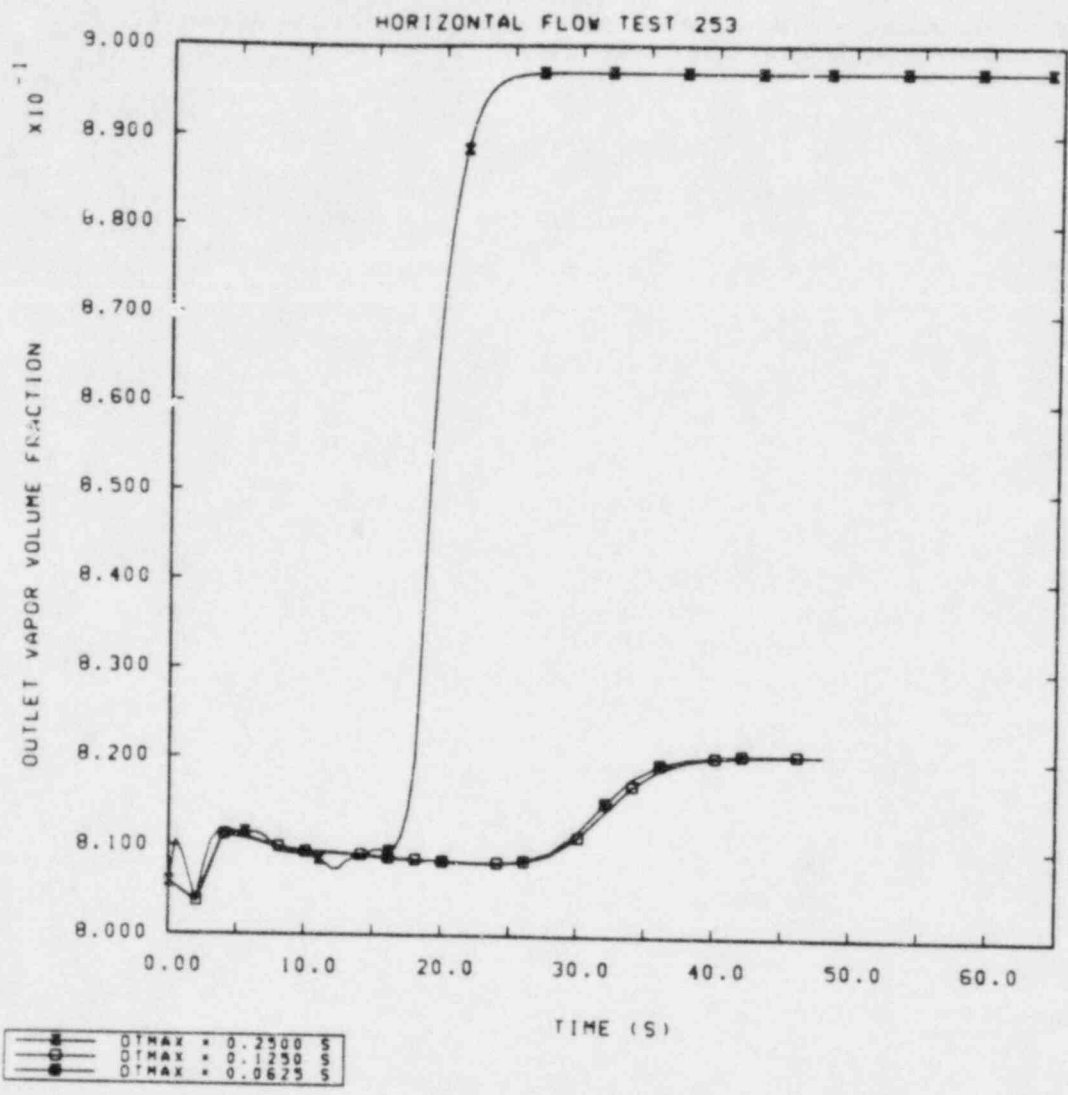
Figure 2.4.3   Outlet Vapor Volume Fraction from
              Converged Steady-State Results:
              Maximum Timesteps of 0.250, 0.125,
              and 0.0625 s

32
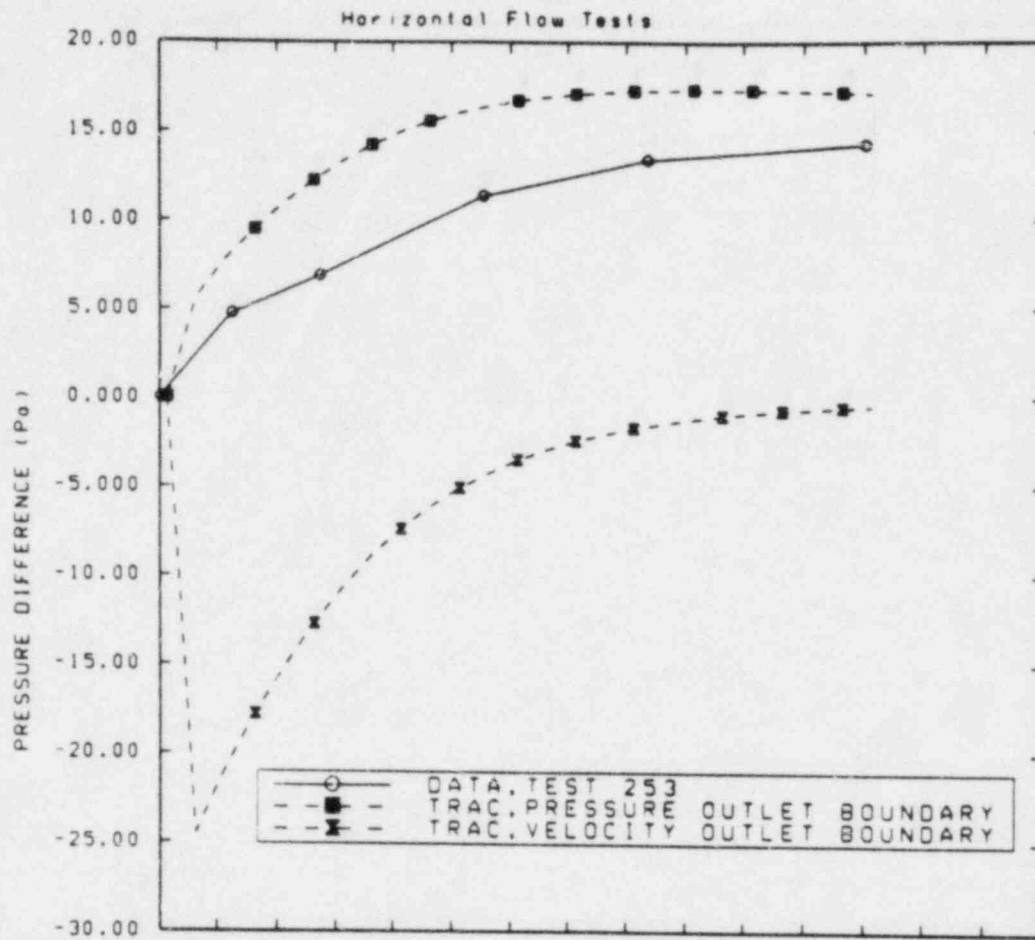
Figure 2.4.4 Pressure Profiles for Test 253 with
Two Outlet Boundary Conditions
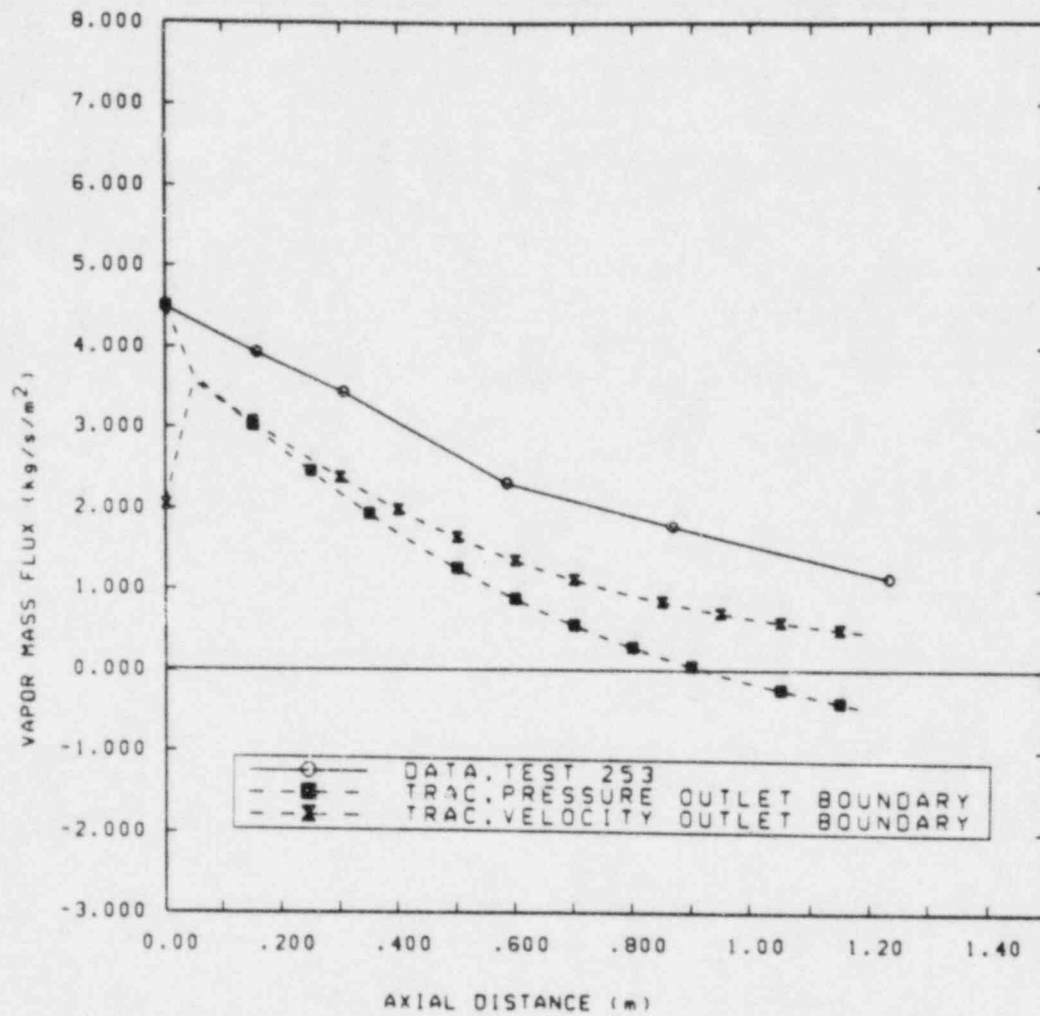
Figure 2.4.5 Vapor Flux Profiles for Test 253 with
Two Outlet Boundary Conditions

34
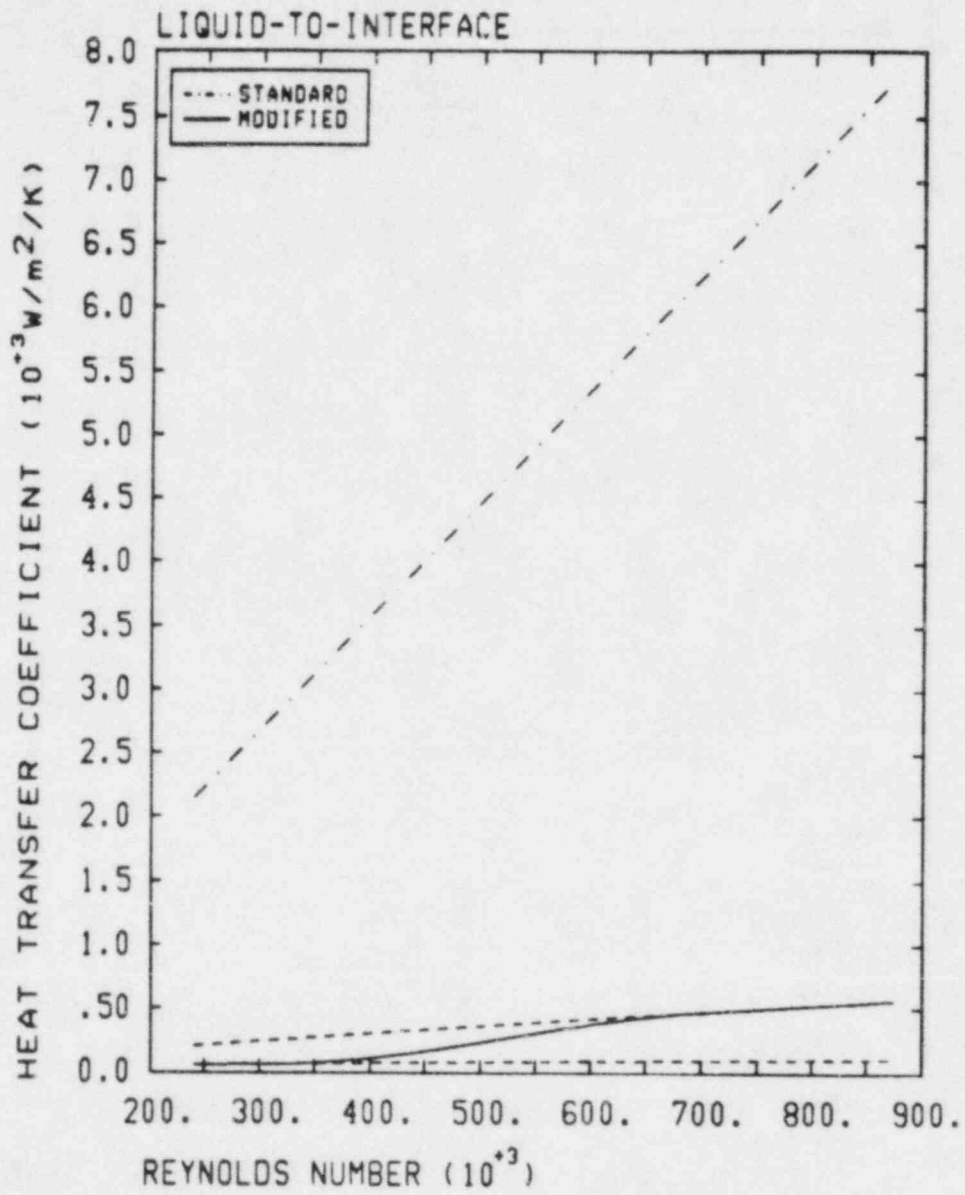
Figure 2.4.6   Standard and Modified Interfacial
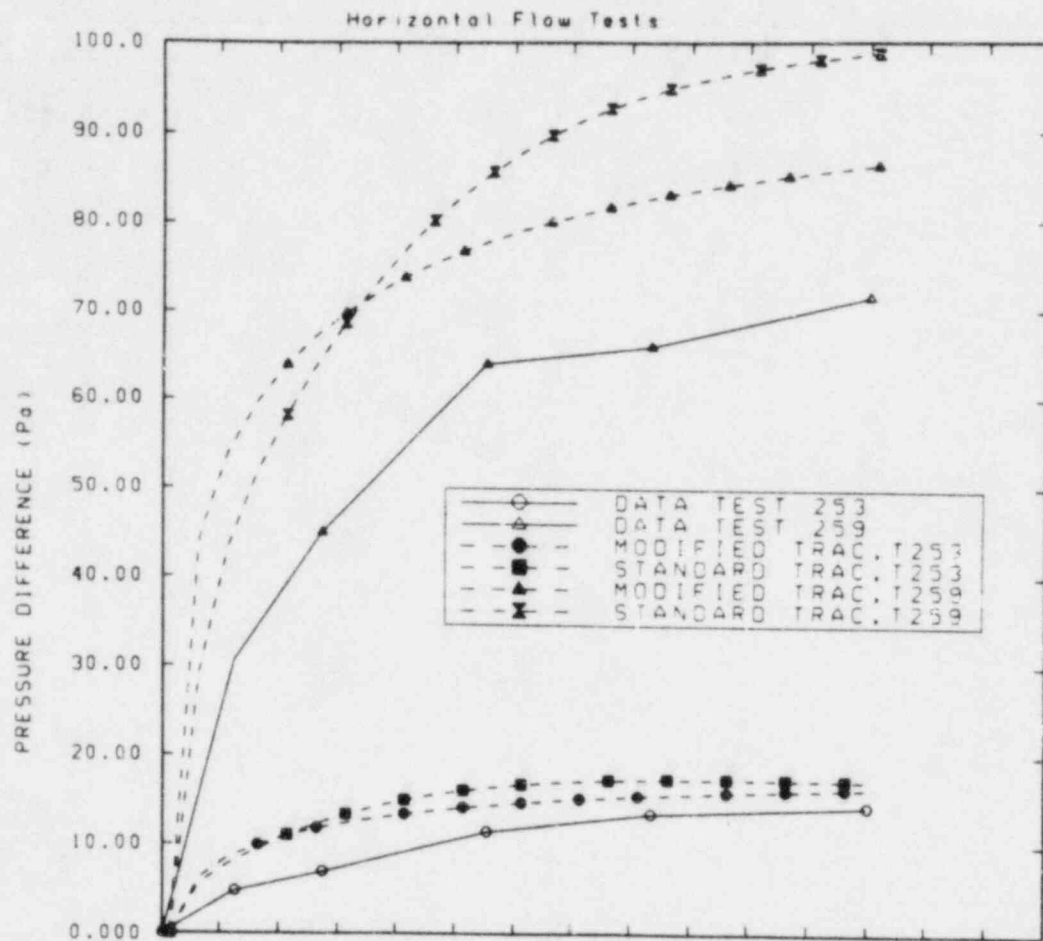Heat Transfer Coefficients

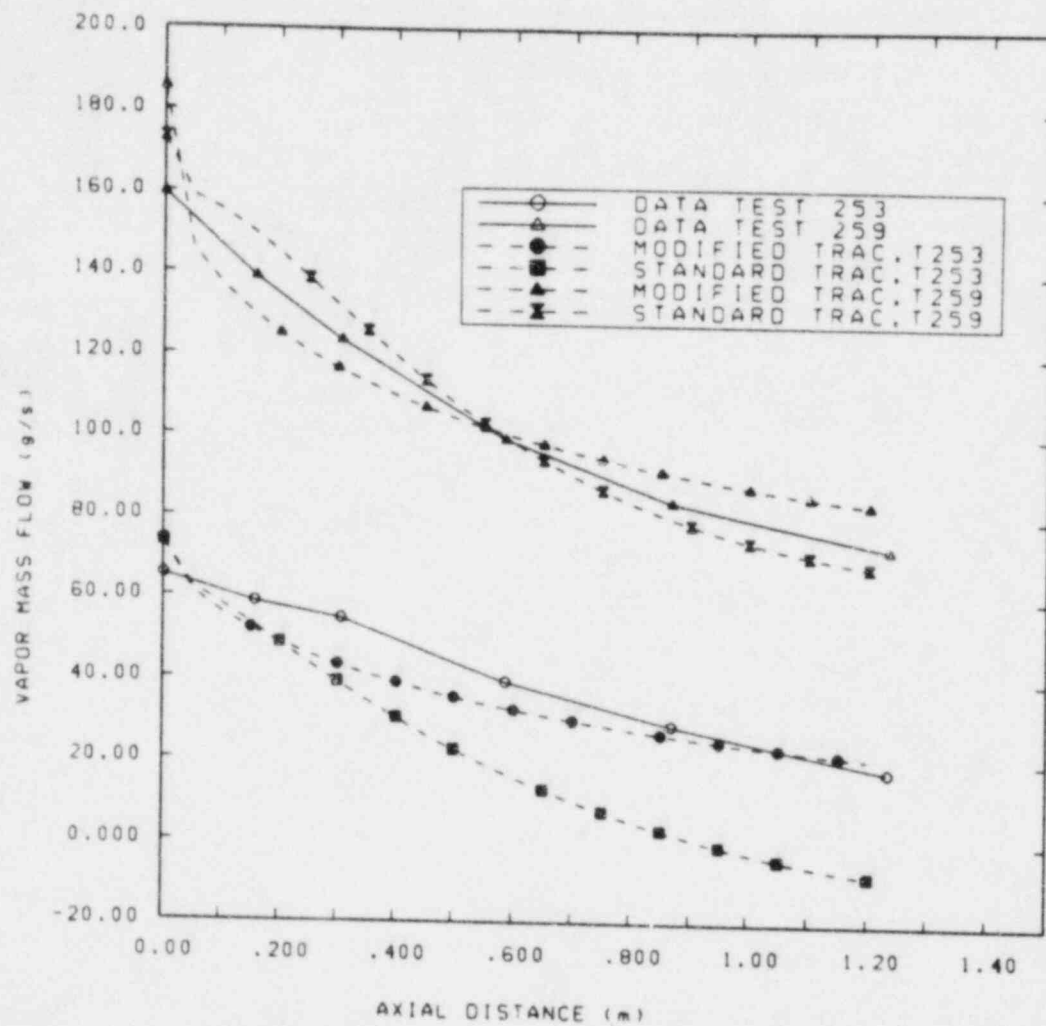Figure 2.4.7 Pressure Profiles for Tests 253 and 259

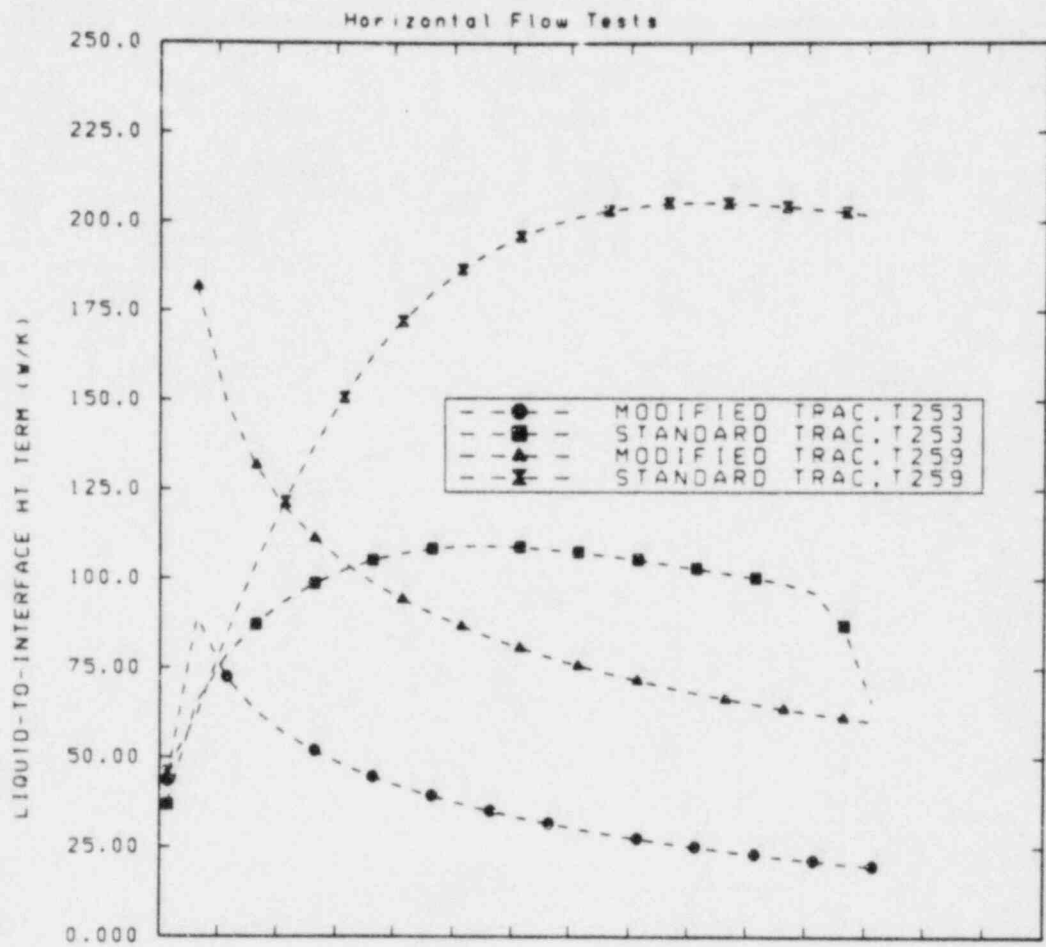Figure 2.4.8   Vapor Flow Profiles for Test 253 and 259

37

Horizontal Flow Tests

250.0
225.0
200.0
175.0
150.0
125.0
100.0
75.00
50.00
25.00
0.000

LIQUID-TO-INTERFACE HT TERM (W/K)

— ● — MODIFIED TRAC.T253
— ■ — STANDARD TRAC.T253
— ▲ — MODIFIED TRAC.T259
— ✕ — STANDARD TRAC.T259

Figure 2.4.9 Interfacial Heat Transfer Terms from
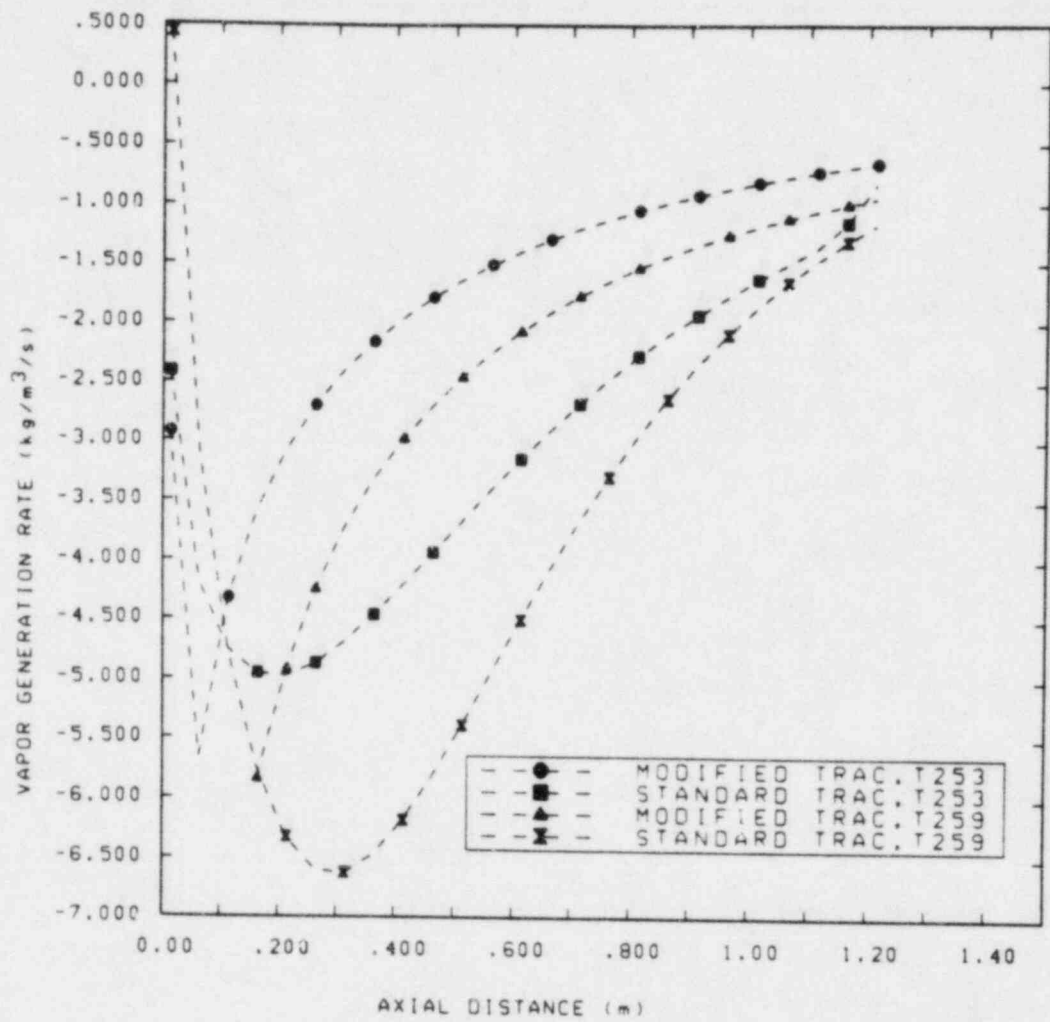Standard and Modified Calculations

38

Figure 2.4.10   Phase Change Rates from Standard and
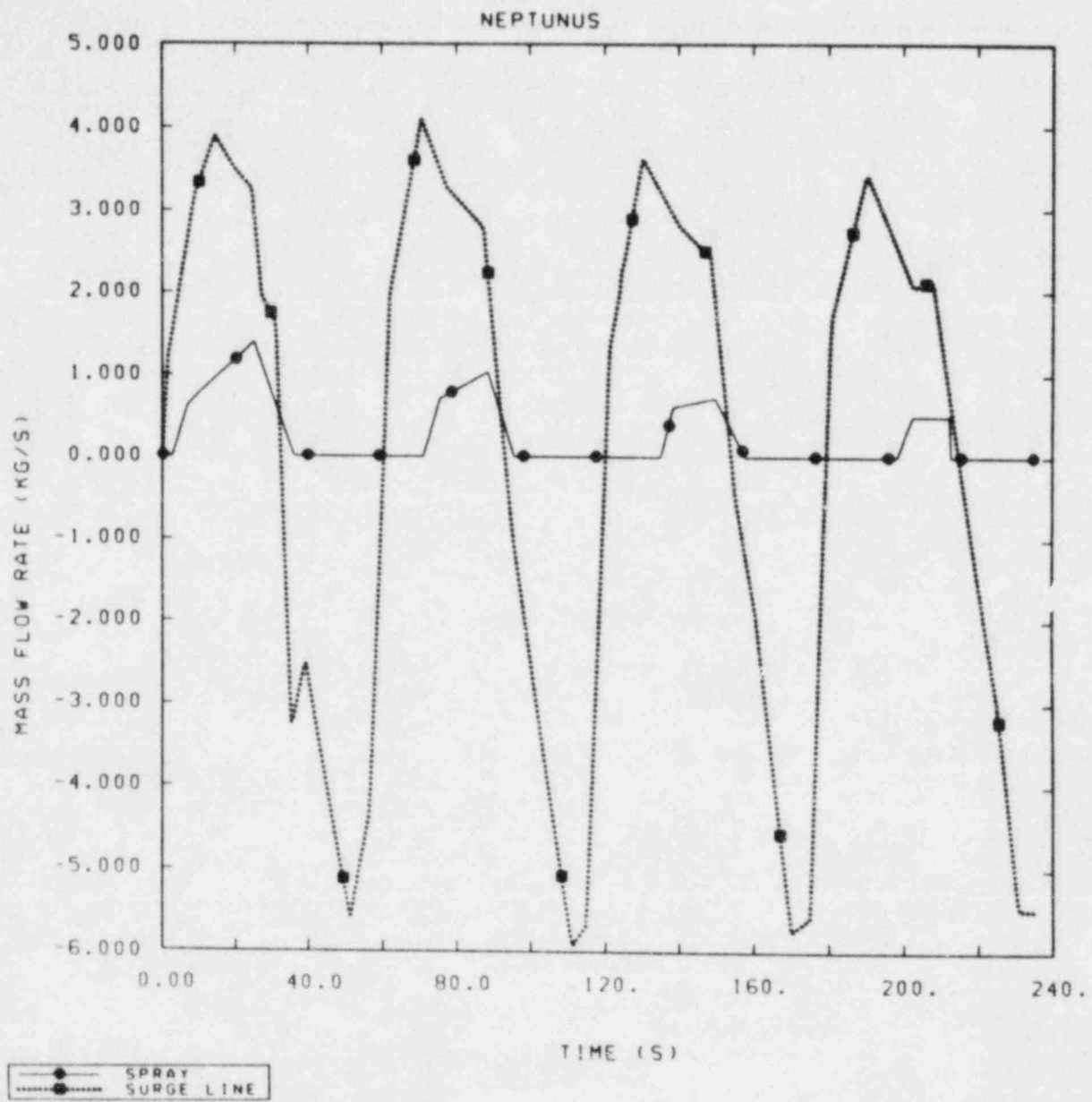Modified Calculations

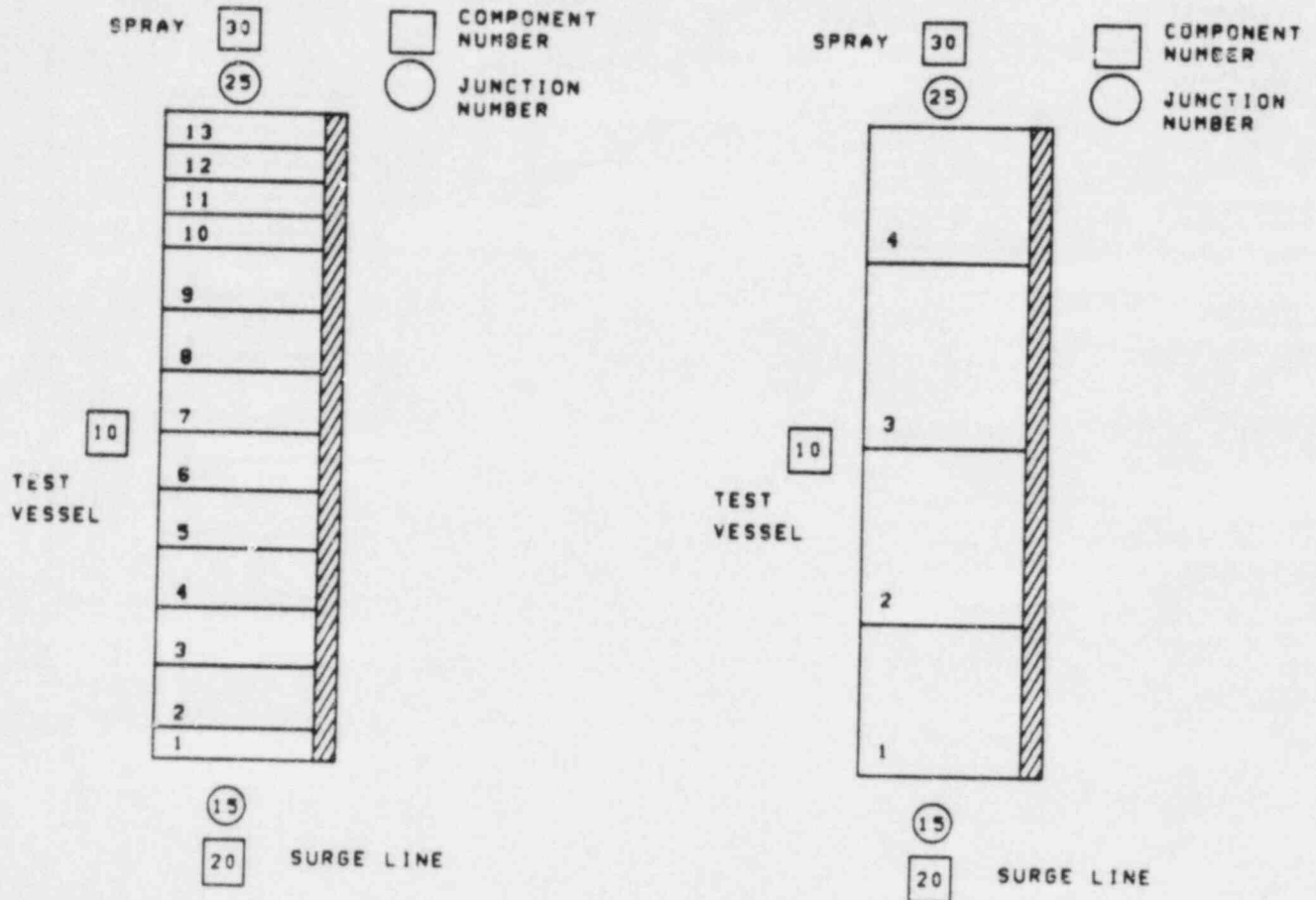Figure 2.5.1 Measured Surge and Spray Line Flows
for NEPTUNUS Test Y05

40

Figure 2.5.2   TRAC-PF1 Noding Diagrams for the
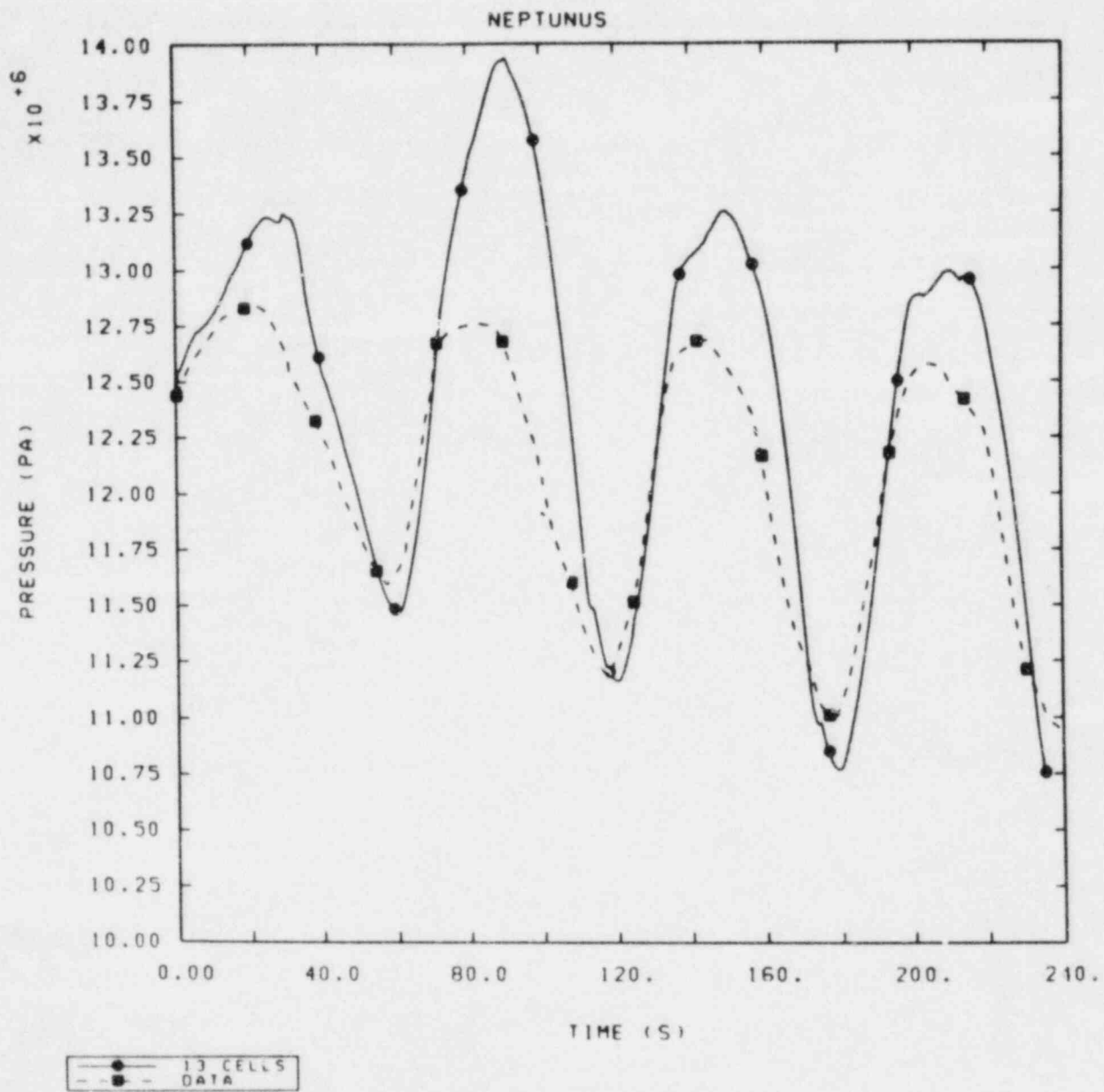NEPTUNUS Test Facility

41

Figure 2.5.3   Calculated and Measured Pressures
for NEPTUNUS Test Y05
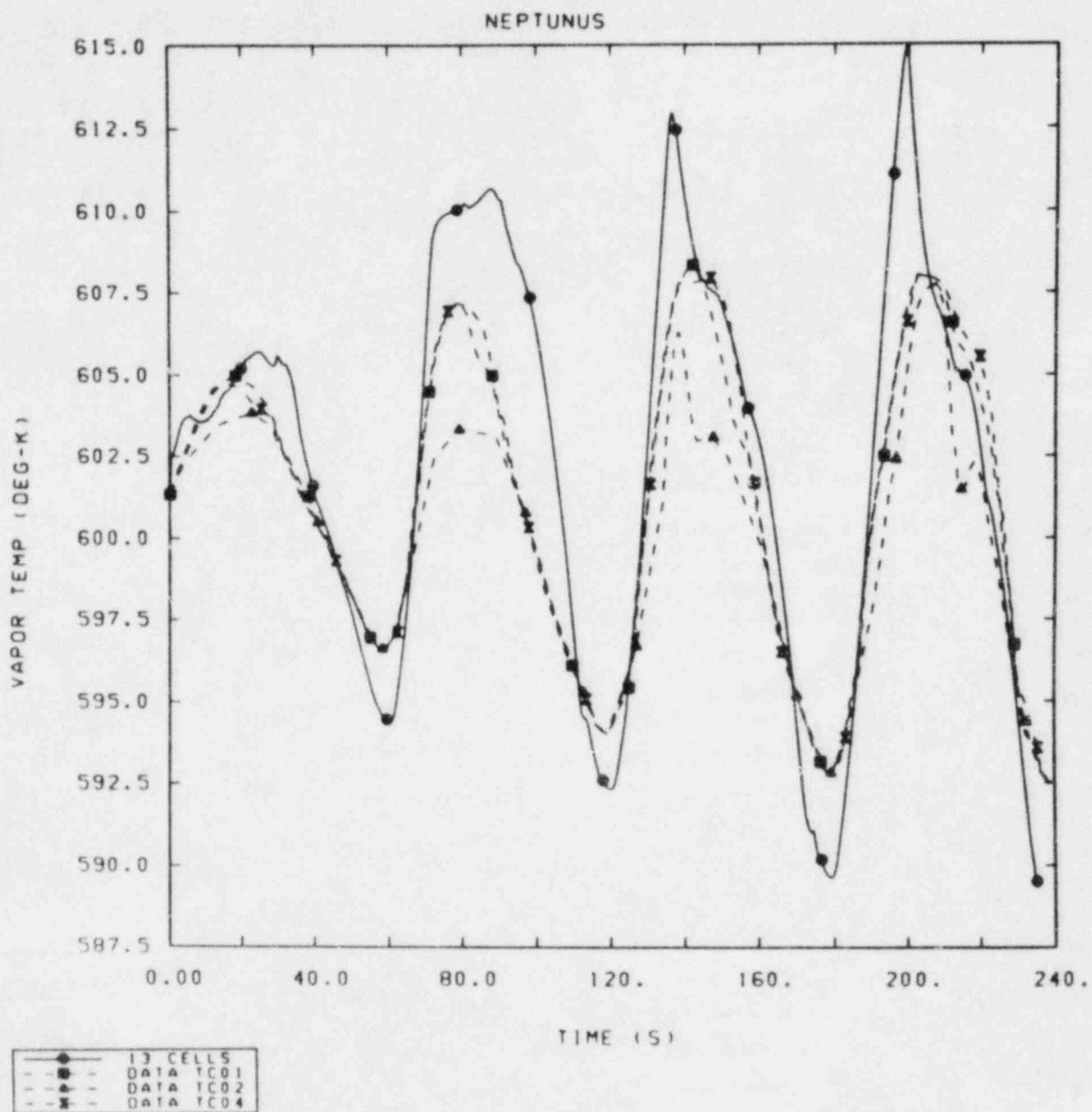
42

Figure 2.5.4   Calculated and Measured Fluid Temperatures
for NEPTUNUS Test Y05

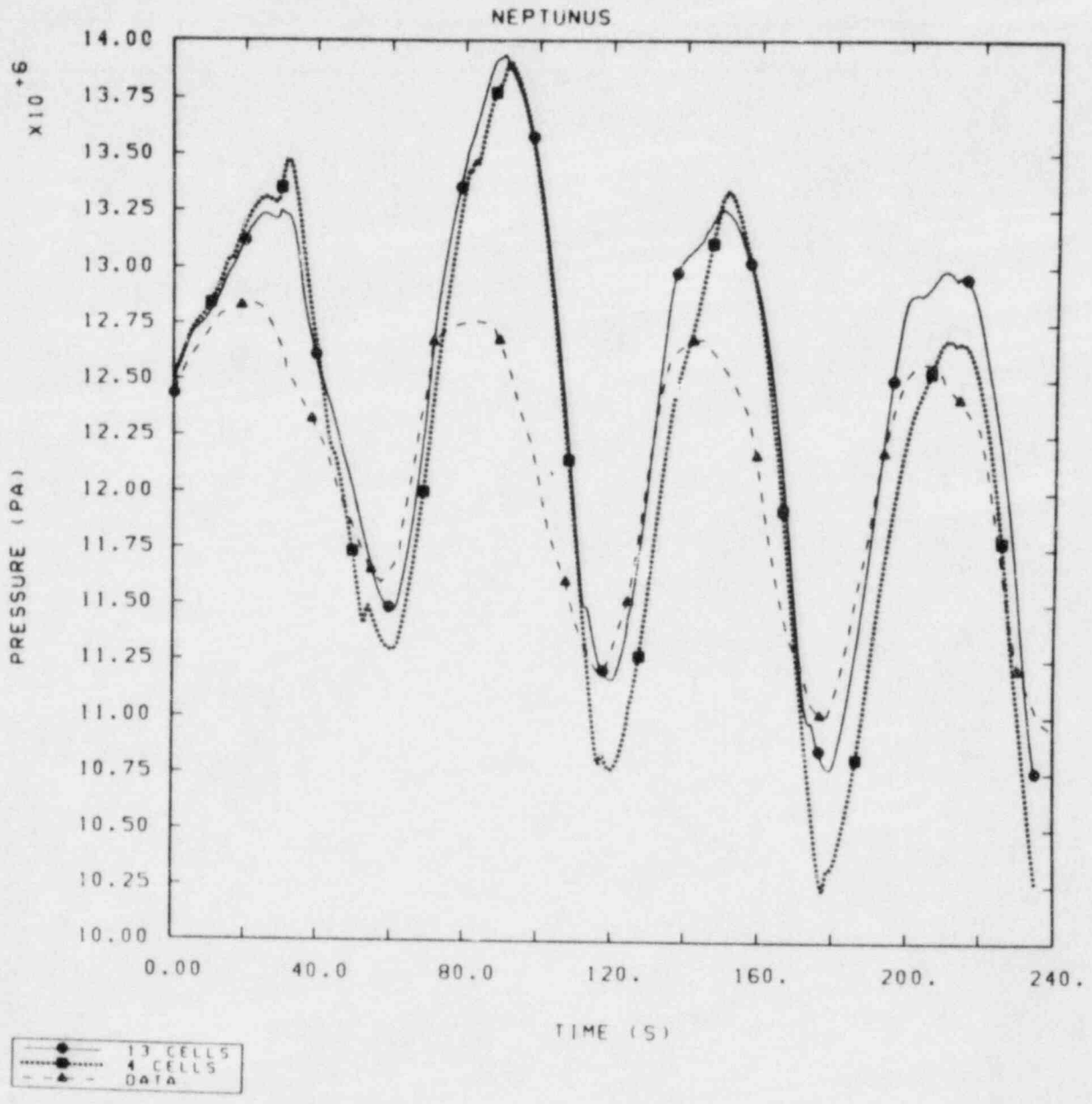43

Figure 2.5.5   Effect of Pressurizer Noding on the
                Calculated Pressure for NEPTUNUS
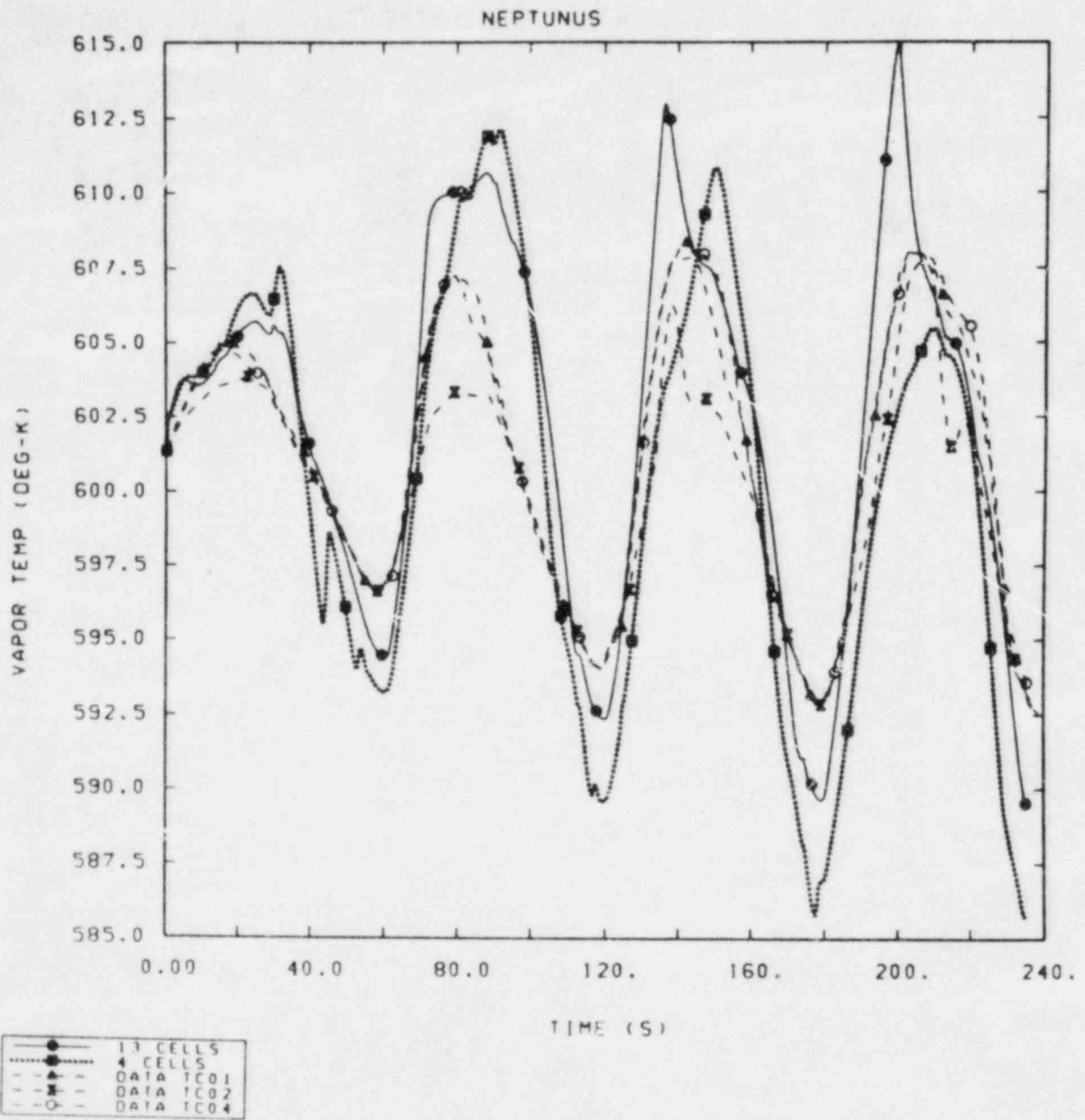   Test Y05

44

Figure 2.5.6   Effect of Pressurizer Noding on the
               Calculated Fluid Temperature for
               NEPTUNUS Test Y05

45

NEPTUNUS

LIQUID TEMP (DEG-K)

620.0
600.0
580.0
560.0
540.0
520.0
500.0
480.0
460.0
440.0
420.0
400.0
380.0
360.0

0.00   40.0   80.0   120.   160.   200.   240.
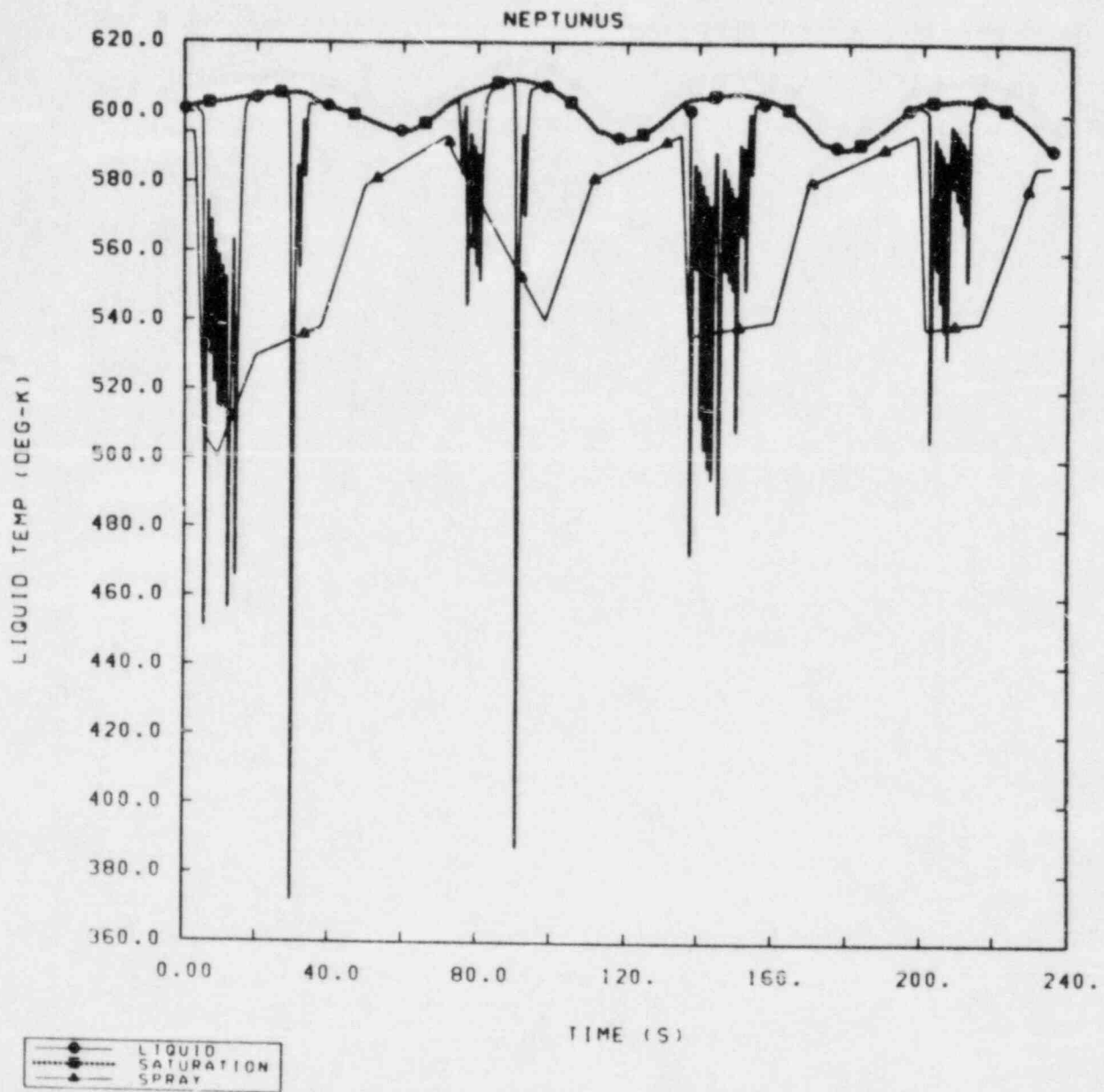
TIME (S)

LIQUID
SATURATION
SPRAY

Figure 2.5.7   Calculated Fluid Temperatures at the Top
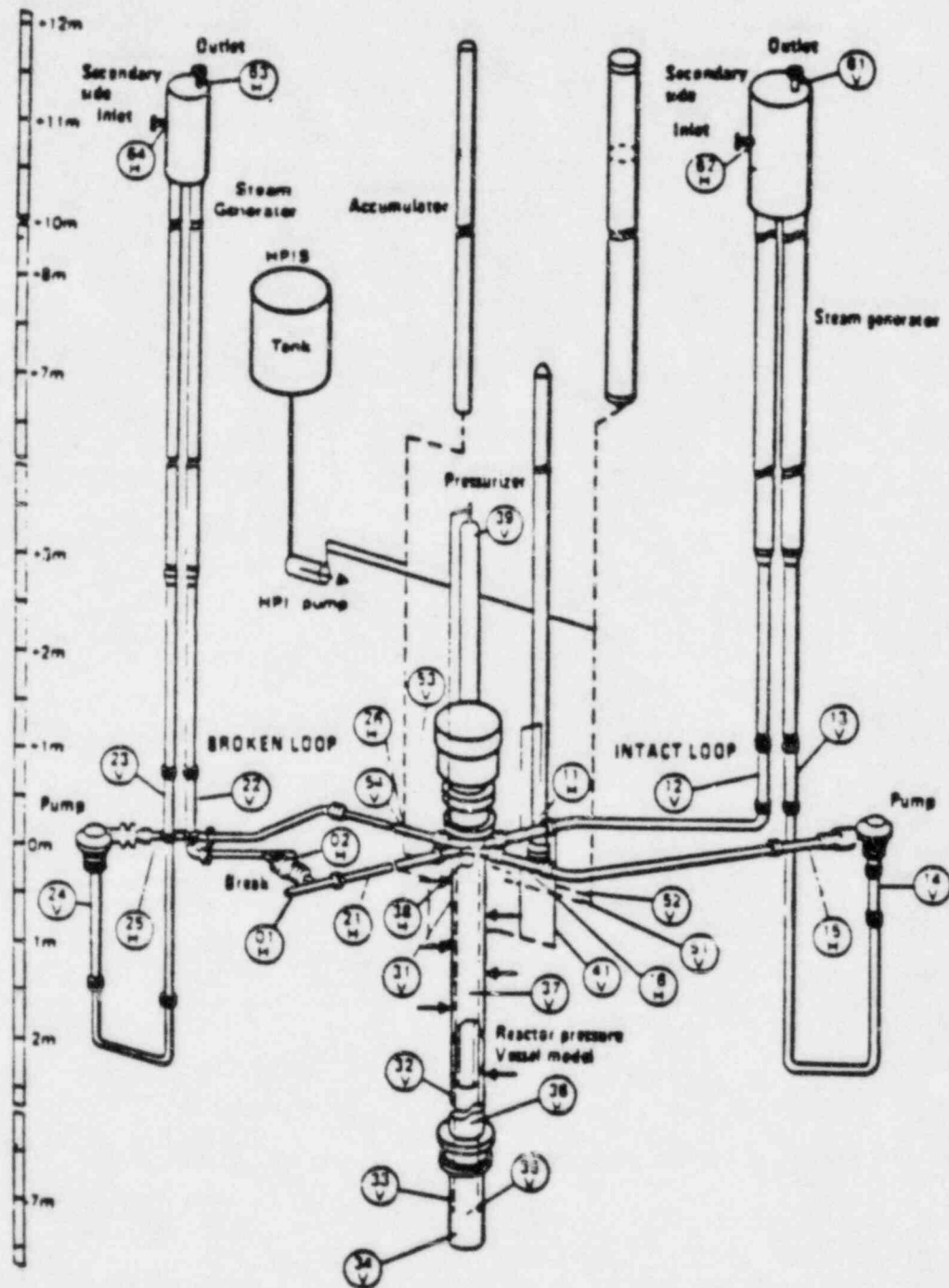of the Pressurizer for the 13 Cell
Pressurizer Model

Figure 2.6.1   LOBI Test Facility
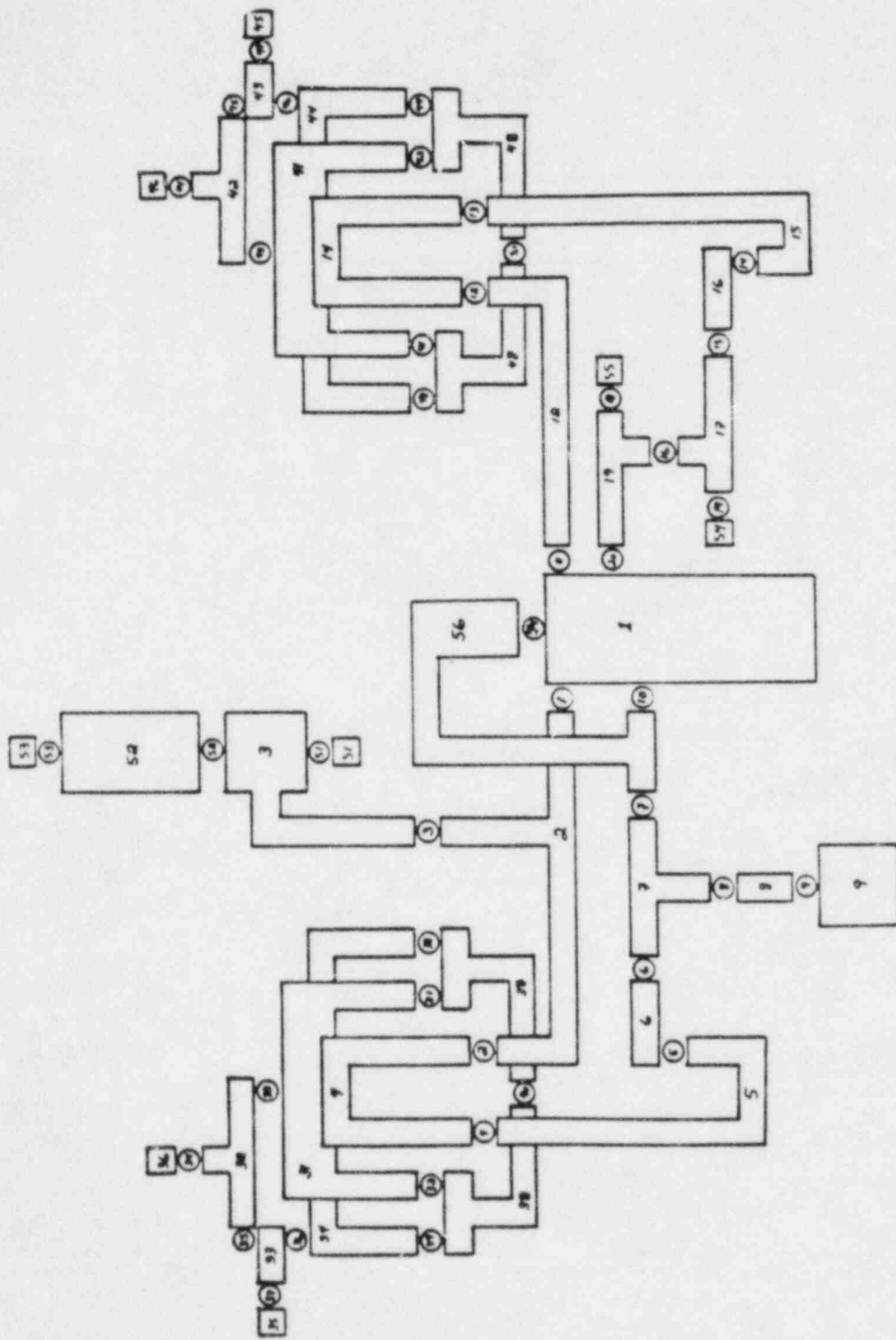
Figure 2.6.2 TRAC-PF1/MOD1 Steady State Nodalization for LOBI Al-04R

48
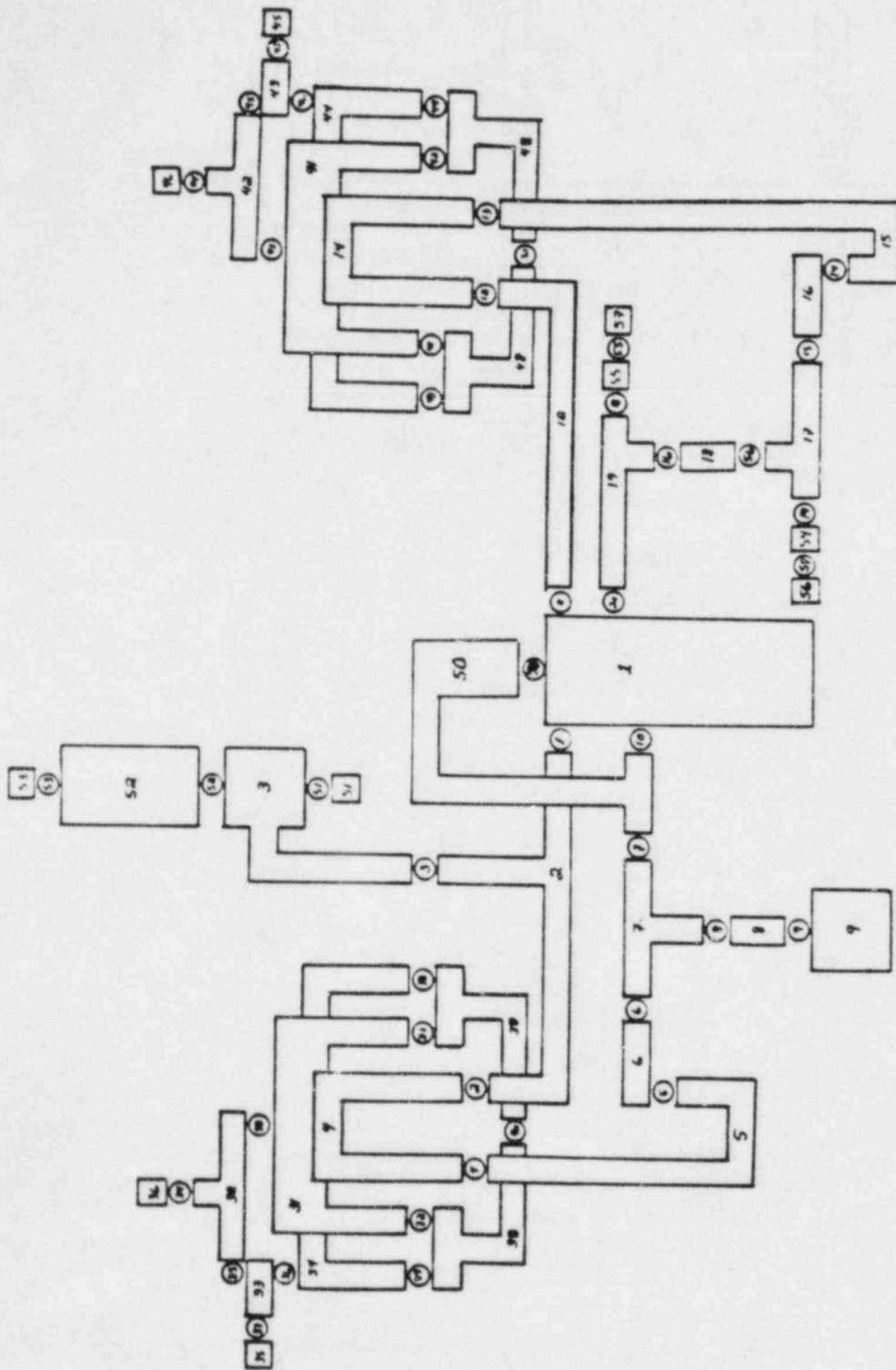
Figure 2.6.3 TRAC-PF1/MOD1 Transient Nodalization for LOBI A1-04R

49

Type II steam generator (broken loop)

Type II steam generator (intact loop)

Special Features:
- Instrumented SG
- Honeycomb insulation
- Pipe heat tracing
- New core

Pressurizer

Vessel

Pump

Hot leg

Hot leg

Cold leg

Break assembly

Pump suction

Pump

Blowdown valve

Condensing coils

Pump suction

Vessel downcomer

Condensate measuring tanks

INEL-A-17 791

Figure 2.7.1 Semiscale MOD-2A Facility

50

Figure 2.7.2 TRAC-PF1/MOD1 Nodalization for Semiscale S-IB-3

3.0 REFERENCES
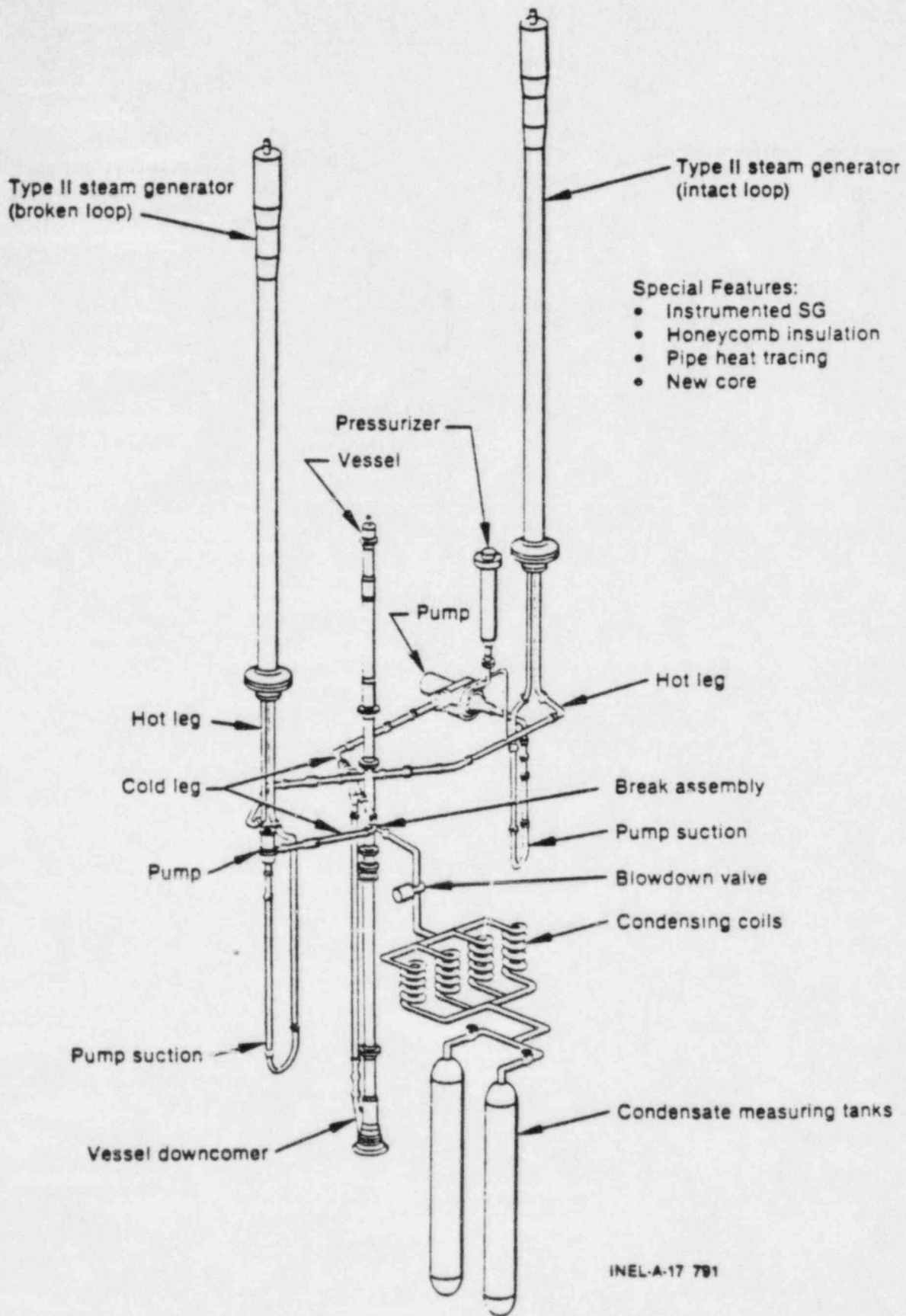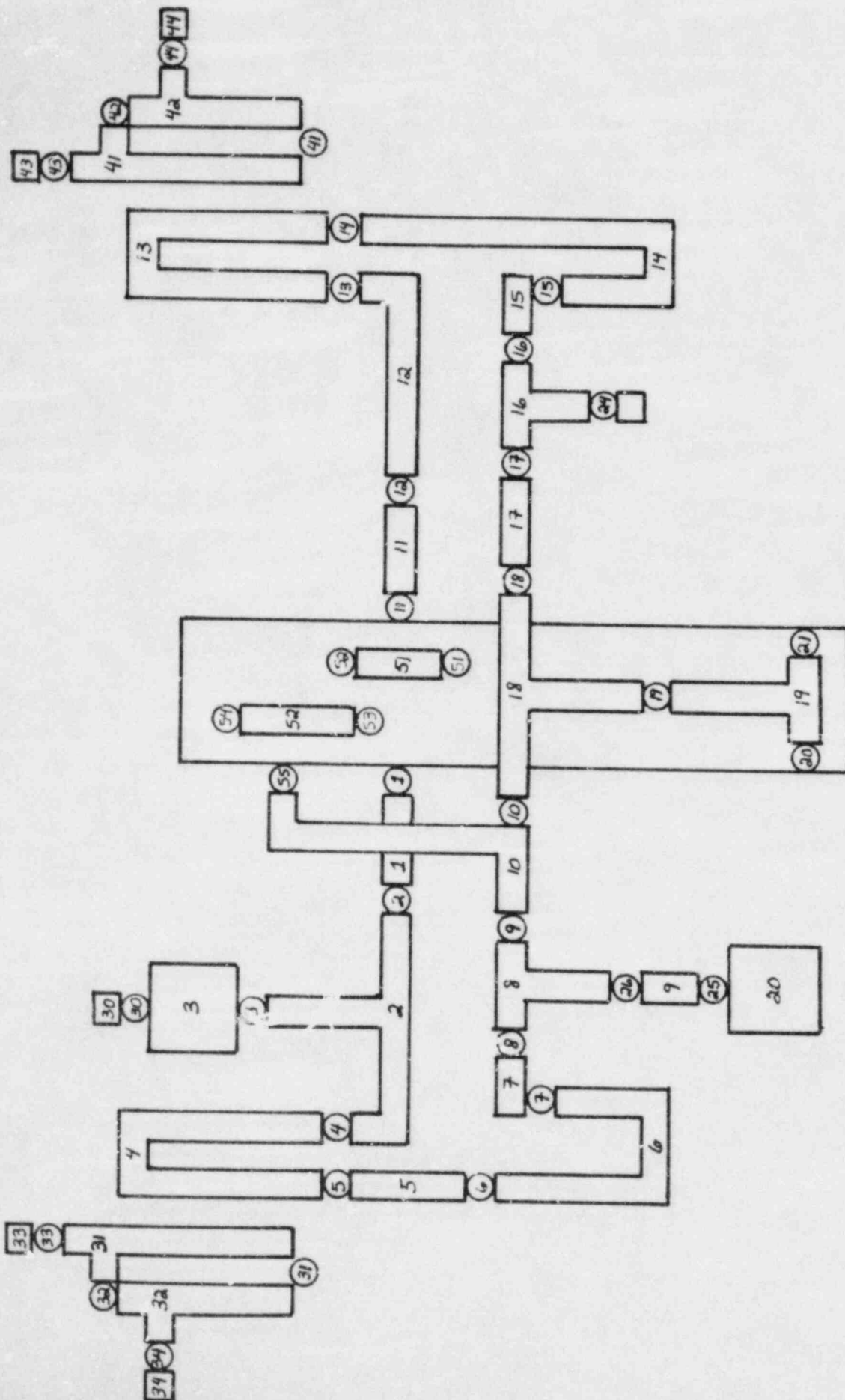
1. TRAC-PF1/MOD1: An Advanced Best-Estimate Computer Program for Pressurized Water Reactor Thermal-Hydraulic Analysis (Draft), Safety Code Development Group, Energy Division, Los Alamos National Laboratory, 1983.

2. S. L. Thompson et al., Thermal/Hydraulic Analysis Research Program Quarterly Report, October-December 1983, NUREG/CR-3329 (Vol. 4 of 4), SAND83-1171, Sandia National Laboratories, March 1984.

3. D. Dobranich and L. D. Buxton, TRAC/PF1/MOD1 Independent Assessment: B&W 19-Tube Once-Through Steam Generator Tests, NUREG/CR-3877P, SAND84-1229, July 1984.

4. H. R. Carter and D. D. Schleappi, Nuclear Once-Through Steam Generator (OTSG and IEOTSG) Loss of Feedwater Flow (LOFW) Test, Report No. 4707, Babcock & Wilcox Co., March 1978.

5. Randall M. Summers, RELAP5 Assessment: B&W 19-Tube Once-Through Steam Generator (OTSG) Loss-of-Feedwater Test, NUREG/CR-3302P, SAND83-2169, December 1983.

6. Flow of Fluids Through Valves, Fittings, and Pipe, by the Engineering Division, Crane Co., 300 Park Ave., NY NY 10022, Technical paper no. 410.

7. B. Brand, R. Kirmse and W. Winkler, OECD-CSNI Standard Problem No. 10: Refill and Reflood Experiments in a Simulated PWR Primary System (PKL), GRS report, December 1979.

8. D. Hein et al, PKL-Small Breaks (Test Series ID): Results of the Steady-State Test PKL ID1 in a Four-Loop Operation with 30 Bar System Pressure, KWU Tech. Rept. No. R 513/18/81, April 1981.

9. S. L. Thompson and L. N. Kmetyk, RELAP5 Assessment: PKL Natural Circulation Tests, NUREG/CR-3100, SAND82-2902, Sandia National Laboratories, January 1983.

10. J. M. McGlaun and L. N. Kmetyk, RELAP5 Assessment: Semiscale Natural Circulation Tests S-NC-2 and S-NC-7, NUREG/CR-3258, SAND83-0833, Sandia National Laboratories, May 1983.

11. I. S. Lim et al., Cocurrent Steam/Water Flow in a Horizontal Channel, NUREG/CR-2289, Northwestern University, August 1981.

12. W. H. Giedt, Principles of Engineering Heat Transfer, Van Nostrand, Princeton, NJ, 1957.

13. H. A. Bloemen, <u>Verification of the Pressurizer Model in RELAP5/MOD1</u>, Energieonderzoek Centrum Nederland, Memo No. 0.375.10 GR 26 (OD 79-24), May 1983.

14. W. Riebold et al., <u>Specifications: LOBI Pre-Prediction Exercise, Influence of PWR Primary Loops on Blowdown (LOBI)</u>, Technical Note No. I.06.01.79.25, Commission of the European Communities, J.R.C.-Ispra, February 1979.

15. L. N. Kmetyk, <u>RELAP5 Assessment: LOBI Large Break Transients</u>, NUREG/CR-3075, SAND82-2525, Sandia National Laboratories, March 1983.

16. L. Piplies and W. Kolar, <u>Quick Look Report on LOBI Test A1-04R</u>, Communication LQC 80-03, Commission of the European Communities, December 1980.

DISTRIBUTION:

U. S. NRC Distribution Contractor (CDSI) (300)
7300 Pearl Street
Bethesda, MD 20014
        300 copies for R4

U. S. Nuclear Regulatory Commission (4)
Reactor Systems Research Branch
Division of Accident Evaluation
Office of Nuclear Regulatory Research
7915 Eastern Avenue
Silver Spring, MD 20910
Attn: Louis M. Shotkin
        Fuat Odar
        R. Landry
        H. S. Tovmassian

EG&G Idaho (6)
Idaho National Engineering Laboratory
P. O. Box 1625
Idaho Falls, ID 83415
Attn: T. R. Charlton
        G. W. Johnsen
        Edna Johnson
        J. C. Lin
        V. H. Ransom
        R. J. Wagner

Thad D. Knight
Dennis R. Liles
Los Alamos National Laboratory (2)
K553 Q-9
Los Alamos, NM 87545

P. Saha, 130
Department of Nuclear Energy
Brookhaven National Laboratory
Associated Universities, Inc.
Upton, New York 11973

N. H. Shah
Babcock & Wilcox Co. (NPGD)
P. O. Box 1260
Lynchburg, VA 24505

Jesse Fell (5)
Deputy Director, Water Reactor Programs
Atomic Energy Establishment
Winfrith
Dorchester, Dorset DT28DH
ENGLAND

```
6400   A. W. Snyder
6410   J. W. Hickman
6417   D. C. Carlson
6420   J. V. Walker
6421   T. R. Schmidt
6422   D. A. Powers
6423   P. S. Pickard
6425   W. J. Camp
6427   M. Berman
6427   C. C. Wong
6440   D. A. Dahlgren
6442   W. A. von Riesemann
6444   S. L. Thompson   (16)
6444   L. D. Buxton
6444   R. K. Byers
6444   R. K. Cole, Jr.
6444   P. N. Demmie
6444   D. Dobranich
6444   M. G. Elrick
6444   L. N. Kmetyk
6444   R. Knight
6444   J. M. McGlaun
6444   J. Orman
6444   A. C. Peterson
6444   W. H. Schmidt
6444   R. M. Summers
6444   S. W. Webb
6449   K. D. Bergeron
3141   C. M. Ostrander   (5)
3151   W. L. Garner
8424   M. A. Pound
```

BIBLIOGRAPHIC DATA SHEET

3 TITLE AND SUBTITLE

Thermal/Hydraulic Analysis Research Program
Quarterly Report January-March 1984   Vol. 1 of 4

4 RECIPIENT'S ACCESSION NUMBER

5 DATE REPORT COMPLETED

MONTH	YEAR
May	1984

6 AUTHOR(S)

S. L. Thompson, Person in Charge

7 DATE REPORT ISSUED

MONTH	YEAR
May	1984

8 PERFORMING ORGANIZATION NAME AND MAILING ADDRESS (Include Zip Code)

Sandia National Laboratories
Thermal/Hydraulic Analysis Division 6444
P. O. Box 5800
Albuquerque, NM 87185

9 PROJECT TASK WORK UNIT NUMBER

10 FIN NUMBER (S)

A-1205 and A-1374

11 SPONSORING ORGANIZATION NAME AND MAILING ADDRESS (Include Zip Code)

Reactor Systems Research Branch
Division of Accident Evaluation
Office of Nuclear Regulatory Research
U. S. Nuclear Regulatory Commission
Washington, DC 20555

12a TYPE OF REPORT

Technical

12b PERIOD COVERED (Inclusive dates)

January-March 1984

13 SUPPLEMENTARY NOTES

14 ABSTRACT (200 words or less)

15a KEY WORDS AND DOCUMENT ANALYSIS

15b DESCRIPTORS

16 AVAILABILITY STATEMENT

17 SECURITY CLASSIFICATION
(This report)

Uncl

18 NUMBER OF PAGES

60

19 SECURITY CLASSIFICATION
(This page)

Uncl

20 PRICE

S